Technical feasibility study for slurry transport of the Atlantis II deep sea mining field - REDACTED

S. Jorna

Delft University of Technology

Section of Dredging Engineering

Final version August 23, 2019

Technical feasibility study for slurry transport of the Atlantis II deep sea mining field - REDACTED

by

S. Jorna

to obtain the degree of Master of Science
at the Delft University of Technology,
to be defended publicly on August 23, 2019

This thesis is confidential and cannot be made public until August 23, 2021

An electronic version of this thesis is available at `http://repository.tudelft.nl/`.

TUDelft

Preface

This study has been conducted at Allseas to complete my Master's program at Delft University of Technology, Faculty of Mechanical, Maritime and Materials engineering, section of Dredging Engineering.

First of all I would like to thank Allseas for giving me the opportunity to perform this study at their facilities and providing me with not one, but two supervisors and a very nice place to finish my graduation.

I would like to thank dr. ir. Sape Miedema in particular, who always provided great insight on specifics of slurry transport and could instantly point to critical points and formulas.
I would also like to thank Thijs and Hayo, for joining my graduation committee.

I would like to thank Vincent & Andrys, my supervisors within Allseas, who have spent countless hours providing feedback and thinking along to come up with solutions.

In addition I would like to thank my colleagues at Allseas for providing a great atmosphere at the office.

Finally I would like to thank my parents and sister for supporting me, not only through this graduation, but throughout my entire life.

Introduction

Due to land mining becoming more expensive and overall less efficient, the mining scope has been expanding to the sea. In the sea a lot of metals can be found in higher grades than on land. The challenge here is that in most cases there are several kilometres of water depth to beat before these metals can be recovered.

A six by ten kilometres wide field of metalliferous mud and clay is located in the Red Sea, next to Saudi-Arabia and Sudan. The field has been named: Atlantis II.

However, due to mining prices not being sufficiently high, the depletion scope of the project was abandoned.

The main research question of the report is: What are the requirements for a feasible concept and how to minimize the power consumption for the transport of non-Newtonian Atlantis II metalliferous slurry, whilst maintaining no clogging of the pipeline?

To provide an answer to this question, several sub-questions were composed. These sub questions are:

- What parameters are most important for the determination of the pressure losses?

- What parameters influence clogging of the pipeline during transport?

- What non-Newtonian model gives the best fit to the data from non-Newtonian Atlantis II samples and tests?

- What pumps are most applicable for transport of the slurry?

- What are the options for component sizing in the hydraulic transport system?

A sensitivity analysis is conducted based on the important parameters. This process is described in this report as follows:

The content of this report is divided in the following chapters, which all help to provide an answer to the research questions:

- Chapter 1: Literature Study
  Consulted and used known literature relevant to solving the following research question is discussed in this chapter:
  - What parameters are most important for the determination of the pressure losses?
  - What parameters influence clogging of the pipeline during transport?

- Chapter 2: Concepts
  Here, concepts are developed, proposed and discussed based on requirements, assumptions and design criteria. Certain main systems of the design are presented along with their sub-systems where in the end, combinations between various subsystems are made based on a morphological overview.

At the end of the chapter, a final design is chosen.

Finally, a discussion is presented, in which a critical view is provided on the assumptions and the calculations. The results are provided and conclusions are drawn based on the results. Recommendations are provided on how to proceed with this project and how the research done can be expanded upon further.

Methodology

The preferred solution is the power consumption required for the system. Power is a multiplication of pressure and velocity. Pressure and velocity can be adjusted to values optimized for this specific study, keeping in mind practical feasibility. As the flow and rotational viscosity meter tests are conducted for few values of concentration[**?**], these values will be expanded upon with a non-Newtonian model, where the parameters depend on the concentration. This way a wider range of values for concentration can be compared. Other typical transport parameters will be added to the model, which has been developed in this thesis, to observe what their influence is on obtaining the desired outcome.

Thereafter, errors are calculated to loop back to the non-Newtonian model, as the fit of the model to the data depends on a few points on the range. Meaning the fit formula can be adjusted.

The pressure calculation will be assessed by the practical feasibility, to see if the outcome of the model is representable for a real-life case.

The methodology is further clarified in figure 1.
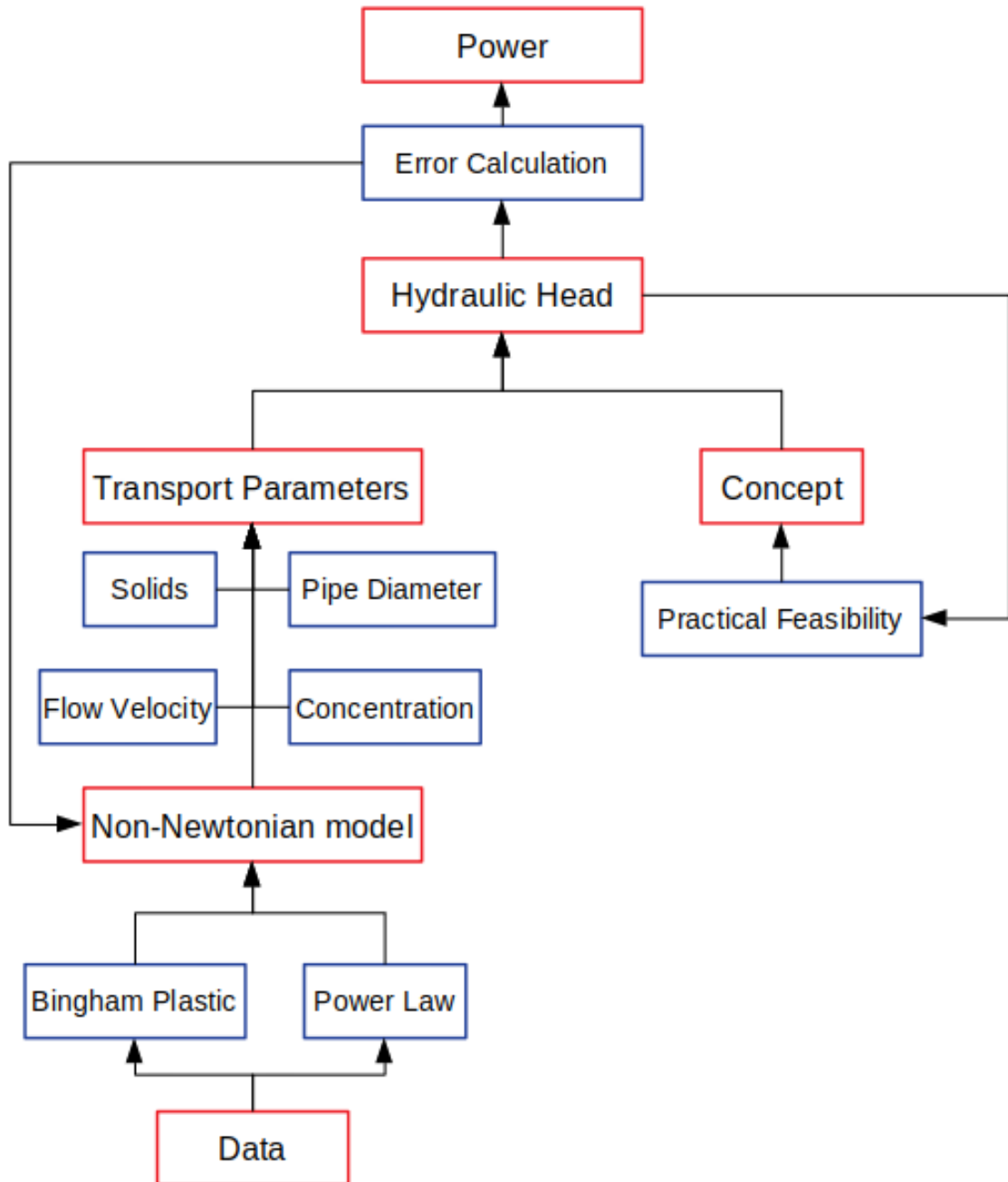
Figure 1: Methodology flowchart

Abstract

Deep sea mining is becoming more popular compared to land mining, as the metal grades for land mines keep dropping and costs are increasing. The Atlantis II Deep is a deep sea mining field of metalliferous muds at a depth of 2200 meter below mean sea level and 115 km from shore in the Red Sea. The area of the field is about 6 km by 10 km with an average depth below seabed of 15m. This field could be exploited by transporting the sediments through a pipeline laid from shore onto the sea bed to the field.

When transported through a pipeline, the sediments exhibit non-Newtonian flow behaviour, which complicates flow predictions. Every change in concentration of solids leads to a different shear stress-shear rate relation, or pressure-flow velocity relation. The sediment is shear thinning, meaning for harder activation in the form of higher flow velocity, the viscosity decreases. From determined concentrations with their shear stress-shear rate relation, parameters for the power law and Bingham plastic model were determined. These model parameters were consequently relayed to concentrations outside of the determined range, to obtain a wider known scope. These models were compared to flow tests of known concentrations and errors between the models and tests were determined, to continue power consumption calculations with the model with the best fit to the data, which is the Bingham plastic model.

Key parameters required to obtain the power consumption are: pipeline diameter, concentration, dilution fluid and the amount of pipelines. Besides the power consumption, flow assurance and practical feasibility are of influence for the concept. Flow assurance is guaranteed by keeping the flow at least slightly turbulent, for a homogeneous distribution of particles in the pipe, while practical feasibility is determined by known pipeline installation projects.

Nomenclature

Abbreviation or symbol	Description	Units
A	Activity	
a	empirical constant, aggregation rate	[-]
AASHTO	American Association of State Highway and Transportation Officials	
b	break-down parameter	[-]
c	$\mu_0 - \mu_\infty$	[Pa s]
CFD	Computational Fluid Dynamics	
cP	centipoise	$0.001 \text{Pa} \cdot \text{s} = 0.001 \frac{\text{N} \cdot \text{s}}{\text{m}^2}$
cSt	centiStokes	$10^{-6} \frac{\text{m}^2}{\text{s}} = \frac{\text{mm}^2}{\text{s}}$
C_v	Concentration of settling particles	[-]
C_{vd}	Delivered Concentration	[-]
D	Pipe Diameter	m
d_{mf}	particle diameter	mm
d_{50}	MASS-median particle diameter	mm
f	Fanning friction factor	[-]
FEM	Finite Element Model	
F_L	empirical coefficient of Durand, $F_L = f(d, C_{vd})$	[-]
g	Gravity	$\frac{\text{m}}{\text{s}^2}$
GSD	Grain Size Distribution	
h	height (of the watercolumn)	[m]
He_B	Hedstrom number (Bingham plastic model)	[-]
I_c	hydraulic gradient of the carrier fluid	$[\frac{\text{m}}{\text{m}}] = [-]$
I_f	hydraulic gradient of the fluid (water)	$[\frac{\text{m}}{\text{m}}] = [-]$
I_m	hydraulic gradient of the mixture	$[\frac{\text{m}}{\text{m}}] = [-]$
K_{BP}	Plastic viscosity (Bingham plastic model)	$[\text{Pa} \cdot \text{s}]$
K_{HB}	consistency index (Herschel-Bulkley model)	$[\text{Pa} \cdot \text{s}^n]$
K_{PL}	consistency index (Power law model)	$[\text{Pa} \cdot \text{s}^n]$
kPa	kilo Pascals	$\frac{\text{kN}}{\text{m}^2}$
LDV	Limit deposit velocity	$[\frac{\text{m}}{\text{s}}]$
L_L	Liquid Limit	[%]
$L_{L,brine}$	Liquid Limit Brine	
$L_{L,DW}$	Liquid Limit Deionized Water	
$L_{L,ker}$	Liquid Limit Kerosene	
M	empirical exponent dependent on the particle size distribution (Wilson-GIW model)	[-]
m_{rz}	empirical exponent Richardson-Zaki	[-]
m	empirical exponent Darby-Melson, Bingham plastic model	[-]
MCA	Multi Criteria Analysis	
MIT	Massachusetts Institute of Technology	
Mp	Megapond	10.000 Pa
n_{HB}	flow index (Herschel-Bulkley model)	[-]
n_{PL}	flow index (Power law model)	[-]
Pa	Pascals	$\frac{\text{N}}{\text{m}^2}$
PDE	Partial Differential Equation	
P_I	Plasticity Index	
P_L	Plasticity Limit	
P	Pressure	Pa

PSD	Particle Size Distribution	
Q	Volumetric Flow Rate	$\frac{m^3}{s}$
Re	Reynolds number	
Re_B	Bingham Reynolds number	[-]
Re_{MR}	Metzner-Reed Reynolds number	[-]
Re_p	Reynolds particle number	[-]
RSCS	Revised Soil Classification System	
S_s	Relative density of solids	[-]
USDA	United States Department of Agriculture	
USCS	Unified Soil Classification System	
v	Velocity	$\frac{m}{s}$
V_{dl}	Deposition Limit Velocity	$[\frac{m}{s}]$
V_m	mean mixture velocity in the pipeline	$\frac{m}{s}$
V_{sm}	Limit stationary deposit velocity (Wilson model)	$\frac{m}{s}$
v_{th}	terminal hindered settling velocity	$\frac{m}{s}$
W_e	Existing water content of the soil	
W_n	Natural water content of the soil	
WRB	World Reference Base for Soil Resources	
w_s	Terminal settling velocity of a particle	$\frac{m}{s}$
α	Particle shape factor	[-]
$\dot{\gamma}$	Shear rate	$[\frac{1}{s}]$
ϵ	Pipe wall roughness	m
λ	Darcy-Weisbach friction factor	[-]
$\lambda_{L,B}$	Darcy-Weisbach friction factor for laminar, Bingham plastic model	[-]
$\lambda_{L,MR}$	Darcy-Weisbach friction factor for laminar, Power law model	[-]
$\lambda_{T,B}$	Darcy-Weisbach friction factor for turbulent, Bingham plastic model	[-]
$\lambda_{T,MR}$	Darcy-Weisbach friction factor for turbulent, Power law model	[-]
μ	Dynamic Viscosity	$Pa \cdot s = \frac{kg}{m \cdot s^2}$
μ_a	Apparent Viscosity	$Pa \cdot s = \frac{kg}{m \cdot s^2}$
μ_s	coefficient for mechanical friction between solids and the pipeline wall (μ_s = 0.4 - 0.44)	[-]
ν	Kinematic Viscosity	$\frac{\mu}{\rho} = \frac{m^2}{s}$
$\xi_{constriction}$	friction factor constrictions	[-]
ξ_{corner}	friction factor corner	[-]
ξ_{flow}	friction factor for the flow	[-]
ϕ	Solids Volume Concentration	[-]
ρ	Density	$\frac{kg}{m^3}$
ρ_c	Carrier fluid density	$\frac{kg}{m^3}$
ρ_s	Solids Density	$\frac{kg}{m^3}$
ρ_l	Liquid Density	$\frac{kg}{m^3}$
τ	Shear Stress	$\frac{N}{m^2}$
τ_w	Wall Shear Stress	$\frac{N}{m^2}$
τ_y	Yield Stress / Shear Strength	$\frac{N}{m^2}$

List of Figures

List of Tables

Contents

1

Literature

In this chapter consulted and used literature are presented in order to gather information on the most efficient way to transport the Atlantis II soil by pipeline. Reading the information in this chapter provides a better understanding of critical parameters and in what way the soil can be prepared leading to the lowest energy consumption and flow assurance of the pipeline.

The next chapter will provide parameters relevant for the Atlantis II field.

1.1. Shear Strength

Every material has its own strength and depending on the material different values for different failure mechanisms. For soils the standard failure mechanism is the shear strength. To indicate, figure 1.1 shows the differences between tensile stress, compressive stress and shear stress acting on a material.
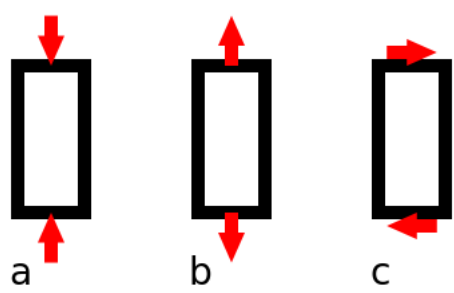
Figure 1.1: a - Compression, b - Tension, c - Shear

Shear strength can be expressed in remoulded state of the soil, or unremoulded state of the soil. For a soil to enter the unremoulded state has to do with pressure and time, this way the soil can build an effective and dense structure of its particles, which will increase its strength compared to its remoulded state. The soil enters the remoulded state after it has been activated/disturbed by any kind of action implying a shear rate and destroying the structure of the soil for sufficient amount of time. This state is much weaker and easier to transport. Shear strength clay soils can be divided in different groups, the divide can be seen in table 1.1.

Table 1.1: Clay Strength Qualification [4]

	Term	Field Identification of Strength for Clays	Shear Strength (kPa)
CLAY	Very Soft	Exudes between fingers when squeezed	<20
	Soft	Moulded by light finger pressure	20-40
	Firm	Moulded by strong finger pressure	40-75
	Stiff	Cannot be moulded - indented by thumb	75-150
	Very Stiff	Indented by thumbnail ('hard'>300 kN/m^2)	>150

1.2. Particle Size Distribution

Soils can be qualified based on their particle size distribution. Depending on the soil type, soils will be characterised by different strength parameters and depending on particle sizes soils can be quantified according to different methods. The following distinctions can be made, shown in table 1.2:

Table 1.2: Soil Classification

Soil Type	USCS Symbol	Grain Size Range (mm)			
		USCS	AASHTO	USDA	MIT
Gravel	G	76.2 - 4.75	76.2 - 2	>2	>2
Sand	S	4.75 - 0.075	2 - 0.075	2 - 0.05	2 - 0.06
Silt	M	<0.075	0.075 - 0.002	0.05 - 0.002	0.06 - 0.002
Clay	C		<0.002	<0.002	0.002

Important to mention when making distinctions of particles based on size, is that silt and clay particles both classify as very small particles, but their properties are very different. Clay particles are longitudinally shaped and have an electrical charge. Whereas silt particles are like sand particles and have more of a round shape with no electrical sensitivity.

1.3. Slurry Transport

1.3.1. Terminal Settling Velocity

Slurry is a mixture of water with solid particles. Depending on the particle size and properties, slurries will exhibit different behaviour for strength, viscosity, pressure losses and settling. All of these parameters can be influenced, therefore the most desired flow can be obtained by tinkering these variables to optimal values.

It is important to determine what amount of solids put into the pipeline will also reach the end. A certain fraction of the particles may settle in the pipeline. For this an equation was formulated by Stokes (with or without viscosity of carrier fluid's influence), Budryck and Rittinger[7], who developed equations for laminar, transitional and turbulent flows respectively for different particle sizes, with viscosity of the carrier fluid.

Stokes equation[7], adjusted to account for the viscosity value of the carrier fluid, can be used for the settling of small particles in a viscous carrier fluid, see equation 1.1. Stokes based his smallest particle size on diameters smaller than 1 mm.

Richardson-Zaki[7] developed an equation to account for hindered settling, see equation 1.2. This equation accounts for increased drag due to proximity of other particles and up flow of liquid as it is displaced by other particles settling, making the process of settling less likely.

$$\text{Stokes}: \quad w_s = \frac{\alpha}{18} \frac{(\rho_s - \rho_c)gd^2}{\eta_a} \tag{1.1}$$

w_s	terminal settling velocity	$[\frac{m}{s}]$
α	particle shape factor	$[-]$
ρ_s	solids density	$[\frac{kg}{m^3}]$
ρ_c	carrier fluid density	$[\frac{kg}{m^3}]$

$$\text{Richardson} - \text{Zaki}: \quad v_{th} = v_t(1 - C_v)^{m_{rz}} \tag{1.2}$$

v_{th}	terminal hindered settling velocity	$[\frac{m}{s}]$
C_v	concentration of settling particles	$[-]$
m_{rz}	empirical exponent: $\frac{4.7\left(1+0.15Re_p^{0.687}\right)}{1+0.253Re_p^{0.687}}$	$[-]$
Re_p	Particle reynolds number: $\frac{v_{ts}d}{v_f}$	$[-]$

1.3.2. Limit Deposit Velocity

The deposition limit velocity is the lowest velocity possible where there is no stratified flow yet, meaning that particles are on the edge of settling, but do not settle yet.

This criterion is extremely important for the flow assurance requirement of the pipeline. Formulas to determine this limiting velocity are developed by Durand, Wilson and MTI - Holland[24]. A differentiation can be made according to different particle sizes, which instigate different transport regimes.

- Homogeneous flow
- Heterogeneous flow
- Sliding bed
- Fixed/Stationary bed

Differentiation between these transport regimes is based on: settling particle size, flow velocity and pipeline diameter.

When dividing flow in different regimes and using separate equations for every regime, care needs to be taken that values expressing the transition from one regime towards the other, might make a sudden jump and will not completely line up with one-another.

The equations proposed by Durand (equation 1.3), Wilson (equation 1.4) and MTI - Holland (equation 1.8) are shown in the numbered equations.[8]

$$\text{Durand}: \quad V_{dl} = F_L \sqrt{2g(S_s - 1)D} \tag{1.3}$$

V_{dl}	deposition limit velocity	$[\frac{m}{s}]$
F_L	empirical coefficient; $F_L = f(d, C_{vd})$	[-]
g	gravity	$[\frac{m}{s}]$
S_s	relative density of solids	[-]
D	pipe diameter	[m]

$$\text{Wilson}: \quad V_{sm} = \frac{8.8 \left[\frac{\mu_s (S_s - S_f)}{0.66} \right]^{0.55} D^{0.7} d_{50}^{1.75}}{d_{50}^2 + 0.11 D^{0.7}} \tag{1.4}$$

V_{sm}	Limit stationary deposit velocity (Wilson model)	$[\frac{m}{s}]$
μ_s	coefficient of mechanical friction between solids and the pipeline wall ($\mu_s = 0.44$)	[-]
D	pipeline diameter	[m]
d_{50}	MASS-median particle diameter	[mm]

$$C_{rm} = 0.16 D^{0.4} d^{-0.84} \left(\frac{S_s - S_f}{1.65} \right)^{-0.17} \tag{1.5}$$

C_{rm}	Relative solids concentration (Wilson model)	[-]
D	pipeline diameter	[m]
d	solids diameter	[mm]
S_s	relative solids density	[-]
S_f	relative fluid density	[-]

$$\text{for}: C_{rm} \leq 0.33$$

$$\frac{V_{dl}}{V_{sm}} = 6.75 C_r^{\frac{\ln(0.333)}{\ln(C_{rm})}} \left[1 - C_r^{\frac{\ln(0.333)}{\ln(C_{rm})}} \right]^2 \tag{1.6}$$

$$\text{for} : C_{rm} > 0.33$$

$$\frac{V_{dl}}{V_{sm}} = 6.75 (1 - C_r)^2 {}^{\frac{\ln(0.666)}{\ln(1-C_{rm})}} \left[1 - (1 - C_r)^{\frac{\ln(0.666)}{\ln(1-C_{rm})}} \right] \tag{1.7}$$

C_{rm}	Relative solids concentration (Wilson model)	[-]
C_{vb}	Concentration in the stratified bed layer	[-]
C_{vd}	Volumetric concentration in the flow	[-]
C_r	$\frac{C_{vd}}{C_{vb}}$	[-]
d	solids diameter	[mm]
V_{sm}	Limit stationary deposit velocity	[$\frac{m}{s}$]
V_{dl}	Deposition limit velocity	[$\frac{m}{s}$]

$$\text{MTI - holland:} \quad V_{dl} = 1.7 \left(5 - \frac{1}{\sqrt{d_{mf}}} \right) \sqrt{D} \left(\frac{C_{vd}}{C_{vd} + 0.1} \right)^{\frac{1}{6}} \sqrt{\frac{S_s - 1}{1.65}} \tag{1.8}$$

d_{mf}	particle diameter	[mm]

These equations do not yet give a relation with the viscosity. Later some have been adjusted in a simplistic way to also account for the viscosity of the carrier liquid by a relative viscosity term. This term stands for the viscosity of the fluid divided by the viscosity of water at 20 °C.

1.3.3. Pressure Gradients - Heterogeneous Flow

A certain pressure gradient is required to transport a mixture, as the mixture loses pressure due to friction. For example: highly viscous fluids lose more pressure due to friction than non-viscous fluids and faster, more turbulent transport requires more pressure per traveled distance than laminar or barely turbulent transport. To determine the pressure gradient required to transport a mixture of water with inert particles, several empirical formulas have been derived depending on a vastitude of parameters. Commonly used equations are the one by Durand and the one by Wilson-GIW. These formulas are shown in equation 1.9 and 1.10 respectively.

$$\text{Durand}: \quad \frac{I_m - I_f}{I_f C_{vd}} = 180 \left(\frac{V_m^2}{gD} \frac{\sqrt{gd}}{v_t} \right)^{-1.5} \tag{1.9}$$

$$\text{Wilson} - \text{GIW}: \quad \frac{I_m - I_f}{C_{vd}(S_s - 1)} = 0.5 \mu_s \left(\frac{V_m}{V_{50}} \right)^{-M} = 0.22 \left(\frac{V_m}{V_{50}} \right)^{-M} \tag{1.10}$$

I_m	hydraulic gradient of the mixture	[-]
I_f	hydraulic gradient of the liquid (water)	[-]
C_{vd}	delivered concentration of solids	[-]
S_s	relative density of solids	[-]
V_m	mean mixture velocity in the pipeline	$[\frac{m}{s}]$
V_{50}	value of V_m at which one half of the solids is suspended in the carrier flow	$[\frac{m}{s}]$
μ_s	coefficient of mechanical friction between solids and the pipeline wall ($\mu_s = 0.44$)	[-]
M	empirical exponent dependent on the particle size distribution	[-]

1.3.4. Rheology

Soils containing large concentrations of clay particles, it's behaviour in flow is non-Newtonian. To characterize non-Newtonian behaviour, the rheology of the mixture has to be determined. Rheology describes the relation between imposed force and resulting deformation and covers both the plastic and elastic properties of materials. For the flow of a non-Newtonian slurry, rheological parameters are important and determine how well the fluid flows in a certain regime, how much settling is resisted for particles of various sizes and how much pressure losses are suffered through the transportation system.

For clay it can be stated that the slurry/soil can be in either remoulded or unremoulded condition. The difference between these two is that unremoulded conditions are not disturbed yet, leading mostly to higher shear strength values. In this state, the material is not in the condition to flow. The unremoulded properties on the other hand, do allow for flow of the material. The strong micro-scale structure of the soil has been broken, now the particles are not connected/intertwined any more leading to a decrease in strength and allowing the material to flow.

The rest of this chapter will continue with the remoulded properties.

- *Shear Rate*
  The shear stress exerted by a non-Newtonian fluid depends on the shear rate or shear-strain rate. In a flow this is the difference in velocity over a different position of height; the velocity gradient. This is only the case for laminar flows, which are unidirectional. Turbulent flows have an overall higher shear rate, as the velocities in the conduit are not unidirectional.

- *Shear Stress*
  Shear stress exerted by the mixture is a fluid property. It depends on the shear rate, and for non-Newtonian fluids, this relation is non-linear. This leads to the viscosity, being a function of the shear stress and shear rate and it not having one value for whatever combination of steady flow conditions.

- *Viscosity*
  Using the apparent viscosity, non-Newtonian behaviour can be expressed in Newtonian behaviour. Care has to be exercised, because every point on the viscosity curve of a non-Newtonian fluid has a different apparent viscosity. See equation 1.11 for the relation between shear stress, shear rate and apparent viscosity.

$$\mu_a = \frac{\tau}{\dot{\gamma}} \tag{1.11}$$

μ_a	apparent viscosity	$[Pa \cdot s]$
τ	shear stress	[Pa]
$\dot{\gamma}$	shear rate	$[\frac{1}{s}]$

To capture non-Newtonian behaviour at various shear rates, expressions which give the shear stress as a function of the shear rate can be used. Some of the more known ones shall be listed here, including their

differences. The viscosity is the shear stress exerted by the fluid divided by the shear rate. These formulas are used for the material in remoulded/flow conditions. See table 1.3 for different non-Newtonian fluid equations and their use cases.

Table 1.3: non-Newtonian fluid equations

Name	Shear Stress	Viscosity	Description
Bingham Plastic	$\tau = \tau_0 + K_{BP}\dot{\gamma}$	$\mu = \frac{\tau_0}{\dot{\gamma}} + K_{BP}$	Bingham Plastic equation assumes a yield stress, but after the shear stress has exceeded τ_0, the fluid starts to flow.
Power Law	$\tau = K_{PL}\dot{\gamma}^{n_{PL}}$	$\mu = K_{PL}\dot{\gamma}^{n_{PL}-1}$	The power law gives a non-linear relation between viscosity and shear rate. A yield stress however is not included, therefore this relation is only used for non-Newtonian fluids without a yield stress.
Herschel-Bulkley (yield power law)	$\tau = \tau_0 + K_{HB}\dot{\gamma}^{n_{HB}}$	$\mu = \frac{\tau_0}{\dot{\gamma}} + K_{HB}\dot{\gamma}^{n_{HB}-1}$	The Herschel-Bulkley relation is used for non-Newtonian fluids with a yield stress and provides a non-linear relation between viscosity and shear rate.

In table 1.3 the following parameters are used:

τ	shear stress	[Pa]
τ_0	yield stress	[Pa]
K_{BP}	plastic viscosity	[Pa ·s]
K_{PL}	consistency index	[Pa ·s^n]
K_{HB}	consistency index	[Pa ·s]
n_{PL}	flow index (Power law model)	[-]
n_{HB}	flow index (Herschel-Bulkley model)	[-]

The following can be derived with respect to the parameters for different non-Newtonian models:

- The plastic viscosity is constant for Bingham plastics and the (apparent) viscosity is constant for Newtonian fluids.

- It is not possible to capture the behaviour of a non-Newtonian fluid over a range of shear stress with one value for the apparent viscosity.

- For high shear rates the apparent viscosity will be nearly equal to the plastic viscosity.

Non-Newtonian fluids exhibit two types of behaviour:

- *Shear Thinning*: For these fluids viscosity decreases as shear rate increases, which means the higher the shear rate, the easier the fluid will flow. Most Non-Newtonian fluids exhibit this behaviour. This leads to the following flow index values for the power law equation: $0 < n < 1$.

- *Shear Thickening*: For these fluids viscosity increases as shear rate increases, which means for higher shear rates, the fluid will behave more like a solid and will give a higher resistance to flow. This leads to the following flow index values for the power law: $n > 1$.

Graphs can be drawn for the rheological models to show the relations more clearly between shear stress and shear rate , and between shear thickening and shear thinning behaviour. For these graphs see figure 1.2.
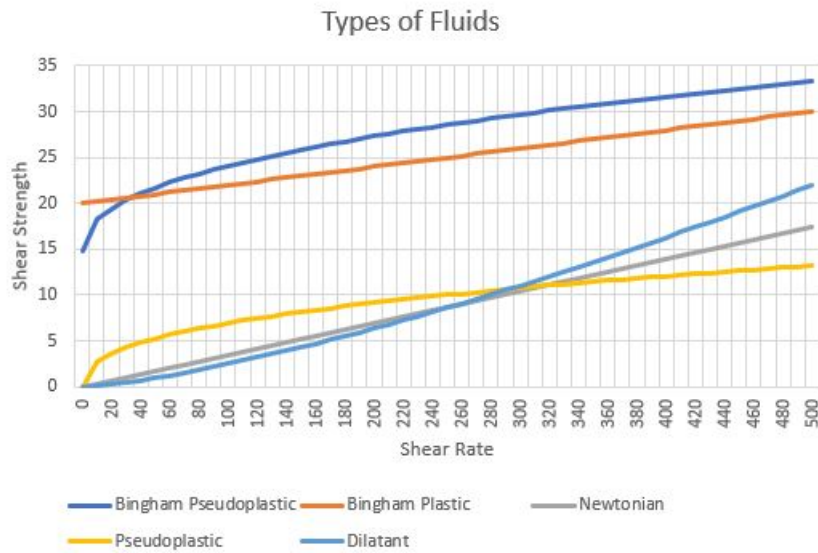
Figure 1.2: Different Rheological Models

Besides the viscosity depending on the shear rate and shear stress, it can also depend on time. When the mixture is exposed to a constant shear rate, viscosity can decrease or increase in time, respectively this is called:

- *Thixotropic*
  The fluid undergoes a decrease in viscosity in time at a constant shear rate. The counter effect of this is that once shearing stops, the fluid will regain some of its strength. This is most notable for the start-up pressure required for the fluid, which in general becomes a significant parameter for the system.

- *Rheopectic*
  The fluid undergoes an increase in viscosity in time at a constant shear rate. But the fluid will also lose some of its strength once the shearing stops.

Viscosity also depends on temperature.

1.3.5. Equations for non-Newtonian fluids

When the parameters are known for the Bingham Plastic and the power law model, pressure losses can be determined according to the equations by Darby-Melson[39] and Metzner-Reed[40].

The Darby-Melson equation consist of two different parts, namely for the laminar and for the turbulent friction factor. The laminar and turbulent friction coefficients are calculated according to the Buckingham-Reiner equation and the Darby-Melson equation respectively, which are shown in the equations 1.12 and 1.13

$$\lambda_{\text{L,B}} = \frac{64}{\text{Re}_\text{B}} \cdot \left(1 + \frac{\text{He}_\text{B}}{6\text{Re}_\text{B}} - \frac{1}{3}\frac{\text{He}_\text{B}^4}{\lambda_{\text{L,B}}^3\text{Re}_\text{B}^7}\right) \tag{1.12}$$

$$\text{with}: \text{Re}_\text{B} = \frac{\rho\text{VD}}{\mu_\text{B}}$$

$$\text{He}_\text{B} = \frac{\rho\text{D}^2\tau_\text{B}}{\mu_\text{B}^2}$$

$$\text{where}: \tau_\text{B} = \text{Bingham yield stress} = \tau_0$$

$$\mu_\text{B} = \text{Bingham viscosity} = \text{K}$$

$$\lambda_{\text{T,B}} = 10^\text{a}\text{Re}_\text{B}^{-0.193} \tag{1.13}$$

$$\text{with : a} = -1.47\left(1 + 0.146e^{-2.9\cdot 10^{-5}\text{He}_B}\right)$$

$$\text{combined Darby \& Melson equation :} \lambda = \left(\lambda_{L,B}^m + \lambda_{T,B}^m\right)^{1/m}$$

$$\text{with :} \lambda_{L,B} = \text{Laminar friction factor - Bingham}$$

$$\lambda_{T,B} = \text{Turbulent friction factor - Bingham}$$

$$m = 1.7 + \frac{40000}{\text{Re}_B}$$

Metzner-Reed based their equation on the power law relation. It will be further clarified below:

$$\text{Power Law :} \tau = K\dot{\gamma}^n$$

Based on the power law parameters, the Metzner-Reed Reynolds number will be calculated, which will be used to calculate laminar-turbulent pressure losses. See equations 1.14 and 1.15 for this determination for respectively the laminar and the turbulent Reynolds numbers.

$$\boxed{\lambda_{L,MR} = \frac{64}{\text{Re}_{MR}}} \tag{1.14}$$

$$\boxed{\lambda_{T,MR} = \left(\frac{D}{\text{Re}_{MR}}\right)^{\frac{1}{3n+1}}} \tag{1.15}$$

$$\text{with :} \text{Re}_{MR} = \frac{\rho V^{2-n} D^n}{8^{n-1} K\left(\frac{3n+1}{4n}\right)^n}$$

$$D = \frac{2^{n+4}}{7^{7n}}\left(\frac{4n}{3n+1}\right)^{3n^2}$$

$$\lambda_{L,MR} = \text{Laminar friction factor - Power Law}$$

$$\lambda_{T,MR} = \text{Turbulent friction factor - Power Law}$$

Both methods calculate the friction factor depending on regime, but the Darby-Melson equation combines both factors to give an estimation of the transition regime and one formula is used for different flow rates.

When the friction factor is known, pressure losses due to friction can be calculated according to the wall shear stress τ_w or the hydraulic gradient of the mixture I_m. Total pressure required depends not only on the frictional pressure losses, but also on hydro-static pressure, static pressure due to the slurry column and a pressure to be maintained for discharge.

When the pressures are known, the power requirement can be approximated by multiplying the pressure required with the flow rate of transport. Derivations of the wall shear stress and pressure are stated in equations 1.16 and 1.17

$$\boxed{\tau_w = \frac{\lambda}{8}\rho v^2} \tag{1.16}$$

$$\boxed{P = \frac{4 \cdot \tau_w \cdot L}{D}} \tag{1.17}$$

$$\text{with :} \tau_w = \text{wall shear stress}$$

$$P = \text{pressure}$$

See equation 1.18 for the pressure expressed in the Darcy-Weisbach friction factor.

$$P = \lambda \cdot \frac{L}{D} \cdot 0.5\rho u^2 \tag{1.18}$$

Buckingham derived an equation for the average flow velocity, which is shown in 1.19. This equation can be rewritten to give a relation for the wall shear stress for the Bingham plastic model. Equation 1.20 shows

how to obtain the wall shear stress by neglecting the $(\frac{\tau_0}{\tau_w})^4$ term, as $\tau_w > \tau_0$ leads to the term $(\frac{\tau_0}{\tau_w})^4$ being negligible.

$$v = \frac{D\tau_w}{8\eta} \left[1 - \frac{4}{3}\left(\frac{\tau_0}{\tau_w}\right) + \frac{1}{3}\left(\frac{\tau_0}{\tau_w}\right)^4 \right] \tag{1.19}$$

$$\tau_w = \frac{4}{3}\tau_0 + \eta_p \frac{8v}{D} \tag{1.20}$$

1.3.6. Dilution
Dilution is the process of adding water or any other fluid to a slurry. Doing this, the concentration of solids is decreased, leading to a lower friction factor during transport (with equal flow rate/velocity) and weaker rheological parameters.

τ	shear stress	[Pa]
τ_0	yield stress or shear strength	[Pa]
K	consistency index	[-]
n	flow index	[-]

When diluting and looking at the Bingham plastic and power law equation, some things can be made clear:

- **Bingham Plastic - parameters**
  - τ_0 is expected to go down as dilution increases, as this is a property solely dependent of the solids, of which the concentration is decreased
  - K_{BP} is also expected to go down as dilution increases, up till the point it reaches the value for water transport

- **Power Law - parameters**
  - n is expected to go towards 1, as more water and less solid concentration means relatively better Newtonian behaviour, which coincides with a Flow Behaviour Index of 1.
  - K_{PL} is expected to go down, until it reaches the value for transport of water.

1.3.7. Salt Precipitation
Water under certain circumstances can only hold a limited amount of salt. The water near the sea floor and the mud, contains high amounts of salt. This can be supported due to the high pressure and temperature near the sea bed. However, once the mud is being transported, temperature and pressure will drop. These two circumstances both influence the salt solubility of the water negatively, meaning salt precipitation can occur. This process means the salt will no longer be dissolved in the fluid, which can lead to negative effects during transport, such as increased pressure requirement and wear. Besides this, the salt crystals or particles will be larger than the particles of the carrier fluid, meaning they are not allowed to settle in the pipeline.
What could be done against salt precipitation is add water to the mixture, so the water to salt ratio increases, meaning that even if the salt solubility of the water drops, there is more water for the salt to be dissolved in.

1.3.8. Thixotropy
The Atlantis II soil is thixotropic, meaning viscosity will keep decreasing the longer it remains in constant shear rate. This also means however, that when the shearing stops, the fluid will regain its lost strength over time.
This can be expressed using the first order equation derived by Moore 1.21[2]:

$$\boxed{\frac{\mathrm{d}\lambda}{\mathrm{d}t} = a(\lambda_0 - \lambda) - b\dot{\gamma}\lambda} \tag{1.21}$$

$$\text{with}: a = \text{empirical constant: aggregation rate}$$
$$b = \text{break-down parameter}$$

A Thixotropic behaviour solver can be added to the Navier-Stokes equations. This is a useful addition when validating non-Newtonian fluid behaviour by Computational Fluid Dynamics calculations. This formula is shown in equation 1.22.
[2]:

$$\tau = \tau_\gamma(\lambda) + \mu(\dot{\gamma}, \lambda)\dot{\gamma} = \lambda\tau_0 + (\eta_\infty(\dot{\gamma}) + c\lambda)\dot{\gamma} \tag{1.22}$$

with : $c = \mu_0 - \mu_\infty$: subscripts standing for shear rate

For colloid based fluids, characteristic values to determine thixotropic behaviour are 10 seconds and 10 minutes after a rotational viscometer test. The values lead to a higher yield stress for the fluid. A visual interpretation can be found in figure 1.3.
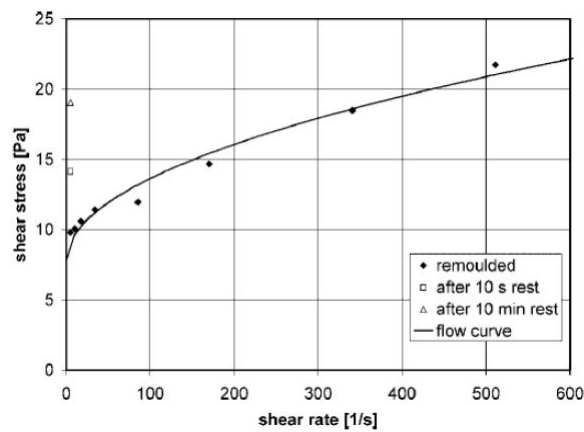
Figure 1.3: Thixotropic behaviour

1.3.9. Start-up Pressure

Thixotropy of the fluid in flow is not important for hydraulic transport as the mixture is in an activated condition, because it will not regain strength. The yield strength of the mixture will increase again once operation is put on hold or stops due to maintenance for example. The remoulded strength found for the mixture on itself is not very high, but due to the thixotropic effect, the yield stress can increase by multiples of its own value. This increase depends on how long the mixture is not activated. That combined with the large length of the pipeline means a much larger start-up pressure is required, than what would be needed for the mixture to flow under normal circumstances. The start-up pressure can be determined by equation 1.23. The very large length of this pipeline makes this a very important parameter to investigate, as the start-up pressure is much larger than the pressure required for the field under normal circumstances.

If the start-up pressure is too large to be designed for, there are practical solutions like flushing the pipeline with water, which can mitigate the effect.

$$p = \frac{4 \cdot \tau_0 \cdot L}{D} \tag{1.23}$$

p	Pressure required	[Pa]
τ_0	Yield stress	[Pa]
L	Pipeline length	[m]
D	Pipeline diameter	[m]

1.3.10. Flow Regime

The flow regime is determined by the Reynolds number, which is shown in equation 1.27. Care needs to be taken, because the Reynolds number is derived for water flows. The Reynolds number of Metzner-Reed however is related to the same values as the Reynolds number for water. For the Bingham Plastic model this

is not the case. Depending on the value of the Reynolds number, the flow will be laminar, in the transition region between laminar and turbulent or turbulent. The Reynolds number itself is dimensionless.

$$\nu = \frac{\mu}{\rho} \tag{1.24}$$

$$v = \frac{Q}{A} \tag{1.25}$$

$$A = \frac{\pi \cdot D^2}{4} \tag{1.26}$$

Using the equations 1.24, 1.25 and 1.26 the Reynolds number can be declared in parameters which can be influenced to adjust the flow regime to whatever regime is desired.

$$Re = \frac{\text{Inertial Forces}}{\text{Viscous Forces}} = \frac{v \cdot D}{\nu} = \frac{v \cdot \rho \cdot D}{\mu} = \frac{\rho \cdot Q \cdot D}{\mu \cdot A} = \frac{4 \cdot \rho \cdot Q}{\mu \cdot \pi \cdot D} \tag{1.27}$$

ν	kinematic viscosity	$[\frac{\text{m}^2}{\text{s}}]$
μ	dynamic viscosity	$[\text{Pa} \cdot \text{s}]$
ρ	density	$[\frac{\text{kg}}{\text{m}}]$
v	velocity	$[\frac{\text{m}}{\text{s}}]$
Q	flow volumetric rate	$[\frac{\text{m}^3}{\text{s}}]$
A	area	$[\text{m}^2]$
D	Pipeline Diameter	$[\text{m}]$

Based on the derivation of the Reynolds number in equation 1.27, it is possible to influence the flow regime to whatever is most suitable for the relevant case.

- Density of the mixture can be decreased by diluting the mixture. Lower density mixtures are less abrasive and need less power to be transported. Opposed to this however, increase in project duration or increase in flow rate should be expected, as the in-situ material is transported in lower concentration.

- Volumetric flow rate of the mixture can be adjusted according to:

    - pressure gradient   - $\frac{\Delta P}{\Delta L}$
    - diameter of the pipe   - D
    - height difference   - ΔH
    - friction factor   - λ (Darcy-Weisbach)

- Viscosity is a fluid related property. However, it can be adjusted, but it is hard to say in certain cases how it will pan out. Adding any adhesive is sure to increase viscosity and any dispersive will lower it, but dilution for example can decrease viscosity. By how much it decreases depends on fluid rheology.

- Pipe diameter is a very important parameter for the flow. Besides the flow regime, it also has a large influence on the friction in the pipe and therefore the head loss due to friction. Overall, smaller pipelines make it easier to transport in the turbulent regime, but come with higher frictional losses.

Different Reynolds numbers refer to different flow regime. Based on practical tests, ranges for the laminar, transitional and turbulent regime have been determined. These values however are not a strict range, as the change from laminar to turbulent flow is not instant. This is a process in which turbulence increases as the Reynolds number increases. The transitional regime is therefore a combination of laminar and turbulent flow, which keeps shifting more and more to turbulent flow as the Reynolds number keeps increasing.
Both flow regimes have their advantages and disadvantages when compared to the other, see table 1.4 for a comparison.

Equations have been derived which can capture both regimes simultaneously. An example is the Churchill[18] equation. Equation 1.28 shows the Churchill equation, which is a formula for calculating the friction factor,

Table 1.4: Flow Regimes Comparison

Laminar Flow	Turbulent Flow
- Individual layers in the flow do not mix, velocity is in the same direction on every position and layers flow parallel to each other and the walls. - Lower Velocities - Unidirectional - Darcy-Weisbach[36][37]: Friction factor - laminar $\frac{64}{Re}$	- Individual layers in the flow mix, velocity is in different directions on various parts of the flow and layers, if there are any, do not flow parallel to each other. - Higher Velocities - Not Unidirectional - Darcy-Weisbach[36][37]: Friction factor - turbulent

independent of the flow regime. Besides being usable in every flow regime, it also gives a very good approximation of the data found through tests.

$$f = 8\left(\left(\frac{8}{Re}\right)^{12} + \frac{1}{\left(\Theta_1 + \Theta_2\right)^{1.5}}\right)^{\frac{1}{12}} \tag{1.28}$$

With:

$$\Theta_1 = \left(-2.457 ln\left(\left(\frac{7}{Re}\right)^{0.9}\right) + 0.27\frac{\epsilon}{D}\right)^{16}$$

$$\Theta_2 = \left(\frac{37530}{Re}\right)^{16}$$

$$\epsilon = \text{Pipe wall roughness} \quad [\text{m}]$$

1.3.11. Drag-, Flow-, and Friction coefficients

For various structures in the pipe, the frictional coefficients can be calculated:

- 180° corner for straight suction mouth:
  $\xi_{\text{corner}} = \sin(\alpha) \cdot \frac{0.44 D^2}{r^2} + 6 \cdot \lambda$

- constriction and dilation of pipe:
  $\xi_{\text{constriction}} = (\frac{A2}{A1} - 1)^2$

- flow losses:
  $\xi_{\text{flow}} = \lambda \cdot \frac{L}{D}$

The total frictional losses can be calculated by equation 1.29. This includes the pressure losses due to pipeline roughness, length and diameter.

$$\Delta P = \sum \xi \frac{\rho u^2}{2} \tag{1.29}$$

ξ	friction coefficient	[-]
ρ	mixture density	$[\frac{kg}{m^3}]$
u	flow velocity	$[\frac{m}{s}]$

1.3.12. Static Pressure Losses

There are pressures, which are not friction related, these are:

- Hydrostatic pressure due to water/brine column
- Hydrostatic pressure due to the slurry column
- Discharge pressure

The discharge pressure is taken as a standard value: 300.000 Pa to maintain pressure at the outlet in order to get the slurry out of the transport system.

The hydro-static pressure due to the water/brine column is a given value and is calculated as can be seen in equation 1.30, this is a positive pressure for the transport system, as this hydro-static column provides pressure on the slurry flow in the pipe.

$$\boxed{P_{hydrostatic} = h_{water} \cdot \rho_{water} \cdot g + h_{brine} \cdot \rho_{brine} \cdot g} \tag{1.30}$$

$P_{hydrostatic}$	Hydrostatic pressure	[Pa]
h_{water}	height of the water column	[m]
ρ_{water}	density of the seawater	$[\frac{kg}{m^3}]$
h_{brine}	height of the brine column	[m]
ρ_{brine}	density of the brine	$[\frac{kg}{m^3}]$
g	gravity	$[\frac{m}{s^2}]$

The hydro-static pressure of the slurry however, which stand for the slurry in the pipe, is a negative pressure, as this provides pressure against the slurry to be pumped up. See equation 1.31 for the equation, on which the concentration/density is of influence.

$$\boxed{P_{static,slurry} = h_{mixture} \cdot \rho_{mixture} \cdot g} \tag{1.31}$$

$h_{mixture}$	height of the mixture column	[m]
$\rho_{mixture}$	density of the mixture	$[\frac{kg}{m^3}]$

1.4. Plasticity & Electrical Sensitivity

Plasticity is the ability of a soil or material to be deformed by forcing, without yielding, and after removal of the force, to remain in this deformed state. Mostly highly plastic soils are soft soils, leading to the relation where cohesion and adhesion are of the same magnitude.

Electrical sensitivity gives an indication of the sensitivity of the fines based on pore fluid changes. Multiple fluids are used to fill the pores and soil responses are measured afterwards. High electrical sensitivity means different behaviour depending on the fluid filling the pores.

1.4.1. Plasticity

Plasticity for a soil is expressed in plasticity index. The plasticity index is the liquid limit minus the plastic limit. The shrinkage limit, liquid limit and the plastic limit can be determined by the Atterberg limit tests, developed by Albert Atterberg and later refined by Arthur Casagrande[35]. The convenient thing about these tests is that the soil does not have to be in its unremoulded state to have its plasticity index determined by these tests. The values in table 1.5 show the plasticity index related to the plasticity of a clay.

- *Shrinkage Limit*
  The shrinkage limit is the water content of the soil, where further increase in water content will not have any effect on reduction of the total volume of the soil. To determine the shrinkage limit, the ASTM International D4943 [23] needs to be performed.

- *Liquid Limit*
  The liquid limit is the water content of clay, where it's behaviour changes from plastic to liquid. However, this change is gradual over a range of water content values and the shear strength of the soil doesn't reduce to 0 at the liquid limit.

Table 1.5: P_I related to plasticity

P_I	Plasticity
0	non-plastic
<7	slightly plastic
7-17	medium plastic
>17	highly plastic

- *Plastic Limit*
  The plastic limit is determined by testing. A thread of the fine portion of the soil is rolled out on non-porous and flat surface. Depending on moisture content of the soil, its behaviour will be plastic or liquid. If behaviour is plastic, the sample can be remoulded and the test can be repeated. The plastic limit is defined as the moisture content where the thread breaks apart with a diameter of 3.2 mm. Whenever it is not possible to roll out a thread of 3.2 mm diameter, the soil is considered non-plastic.

- *Liquidity Index*
  The liquidity index of a soil is used to scale the water content to its limit. See equation 1.32 for the formula which one can calculate the Liquidity index with.

$$L_I = \frac{W_n - P_L}{L_L - P_L} \tag{1.32}$$

W_n	Soil natural water content	[-]
P_L	Plastic limit	[-]
L_L	Liquid limit	[-]

- *Plasticity Index*
  P_I measures the plasticity of the soil. To calculate the P_I, see equation 1.33

$$P_I = \frac{L_L}{P_L} \tag{1.33}$$

P_I	Plasticity index	[-]

Soils with high P_I are clayey, soils with lower P_I are silty and soils with a P_I of 0 contain barely any clay or silt.

- *Consistency Index*
  C_I signifies the firmness of the soil, equation 1.34 determines the consistency index.

$$C_I = \frac{L_L - W_e}{L_L - P_L} \tag{1.34}$$

W_e	Soil existing water content	[-]
C_I	Consistency index	[-]

Soil near the liquid limit will have a consistency of about 0, while soil near the plastic limit will have a consistency of about 1.

- *Activity*
  Activity shows how reactive a soil is to change in water content. Soils with high activity show large

volume changes with relatively small changes in water content and vice versa. See equation 1.35 on how to calculate the activity of a soil.

$$A = \frac{P_I}{\% - \text{Clay}}$$ (1.35)

| A | Activity of the soil | [-] |
| %-Clay | Percentage of clay sized particles (<2μm) | [-] |

Activity for clay is normally in the range of 0.75 - 1.25. Clay with activity below 0.75 is called inactive and clay with activity above 1.25 is called active.

1.4.2. Electrical Sensitivity
Based on the liquid limits of the soil containing brine, deionized water and kerosene with different contents, conclusions are drawn. This method is called the Revised Soil Classification System [25], as opposed to the Unified Soil Classification System or the European Soil Classification System, which are more known and more commonly used, but also older.
The Revised Soil Classification System is used especially for the Atlantis soil to find a correlation with other soils, based on the electrical sensitivity, to draw conclusions with respect to the plasticity. This method is specifically designed to characterize the behaviour of fines in soils.

1.5. Pumps
Two of the most used pumps types are centrifugal pumps and positive displacement pumps. Specific fluid properties are also handled better by one than by the other. At the end of this chapter a table is shown, showing pros and cons of both designs.
In the final concept the most efficient pumps for the requirements of lowest power consumption and flow assurance of the pipeline are chosen based on discussed literature here.

1.5.1. Fluid Properties
Pumps can be chosen based on properties of the fluid that needs to be transported. Important factors which affect this decision are:

- *Acidity and Chemical Composition*
  Corrosion and acidity can degrade the pump and will influence the chosen material

- *Temperature*
  Usually, temperatures of up to 100° C have to be considered for pump materials, expansion, mechanical seal components and packing materials.

- *Solids concentration/particle sizes*
  Abrasive liquids, like slurries of water and particles, influence pump selection. Prevention of clogging and premature failure depends on: particle size, hardness and the volumetric percentage of solids.

- *Specific Gravity*
  The specific gravity of a fluid is the ratio of the fluid density to that of the water under specified conditions. Specific gravity affects the energy required to lift and move the fluid and therefore influences the pumps power requirement.

- *Vapour Pressure*
  Vapour pressure is the pressure exerted by a liquid in order to change its phase from liquid to vapour. It depends on the liquid's chemical and physical properties.
  If the pressure in the pump drops below the vapour pressure, the liquid will boil and small bubbles of boiled water will evaporate against the pumps impeller or piston/plunger/diaphragm and create powerful shock waves, which will damage the pump. Therefore this needs to be taken into account for the wear on the pump.

- *Viscosity*
  Viscosity of the fluid has to be known at the lowest pumping temperature. High viscosity fluids result in reduced centrifugal pump performance and an increased pump power requirement. Of particular importance are the suction side line losses when pumping viscous fluids.

1.5.2. Pump Curves - Positive Displacement vs Centrifugal pumps

Comparing centrifugal pumps to positive displacement pumps, the easiest way to draw a comparison is to compare performance of different parameters in different conditions. With the following sections and graphs the differences will be clear.

Pressure - Flow Rate

As shown in figure 1.4 differences in flow compared to pressure become clear. Centrifugal pumps have a varying flow rate, dependent of pressure, whereas PD pumps have a constant flow, regardless of pressure.
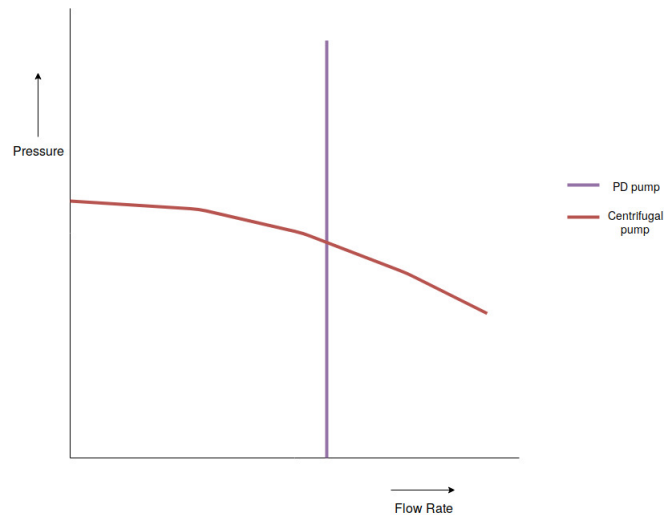
Figure 1.4: Pressure relative to Flow Rate for centrifugal and positive displacement pumps [20]

Flow Rate - Viscosity

For PD pumps the flow rate increases with increasing viscosity, as shown in figure 1.5. This is due to the fact that the clearances are filled by the viscous fluid and back flow between them is less likely. On the other hand, the centrifugal pump loses flow as it handles more viscous fluids.

Furthermore, higher viscosity also results in higher discharge line friction losses, which is not shown in the graph presented here.
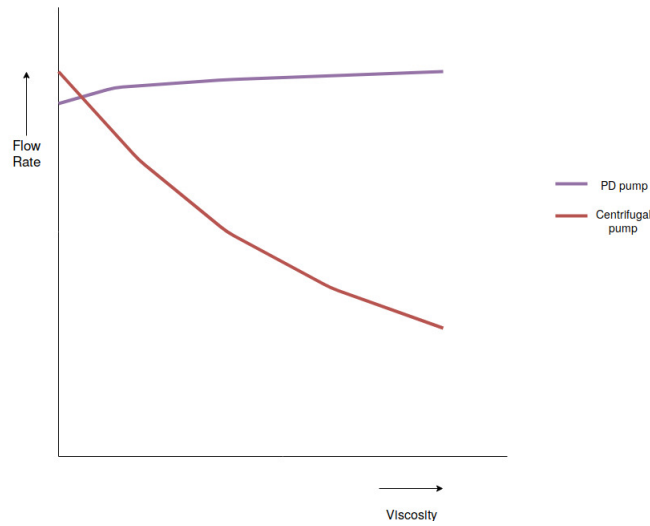
Figure 1.5: Flow Rate relative to Viscosity for centrifugal and positive displacement pumps [20]

Efficiency - Pressure
Figure 1.6 illustrates mechanical efficiency as a function of pressure. As can be seen, there is an optimum pressure for centrifugal pumps and any deviation from this optimum leads to a fast decrease in efficiency. On the other hand, pressure variations have little effect on PD pumps.
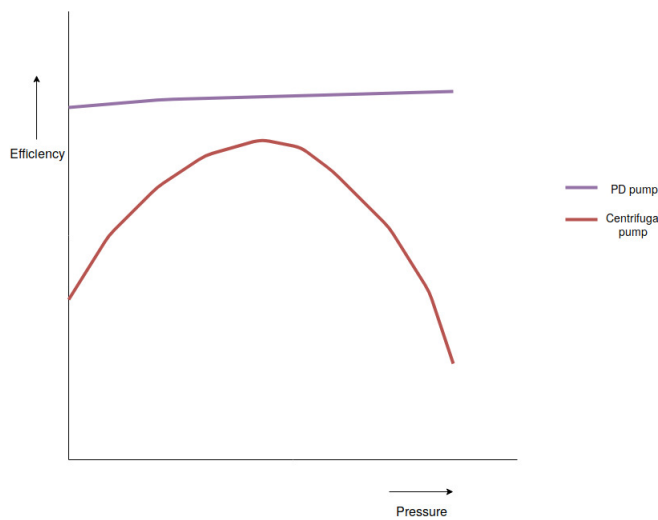
Figure 1.6: Efficiency as a function of Pressure for centrifugal and positive displacement pumps [20]

Efficiency - Viscosity
Figure 1.7 presents the influence of viscosity on pump efficiency. Efficiency decreases for centrifugal pumps, due to frictional losses in the pump. For PD pumps there is often an increase, followed by a slow decline.
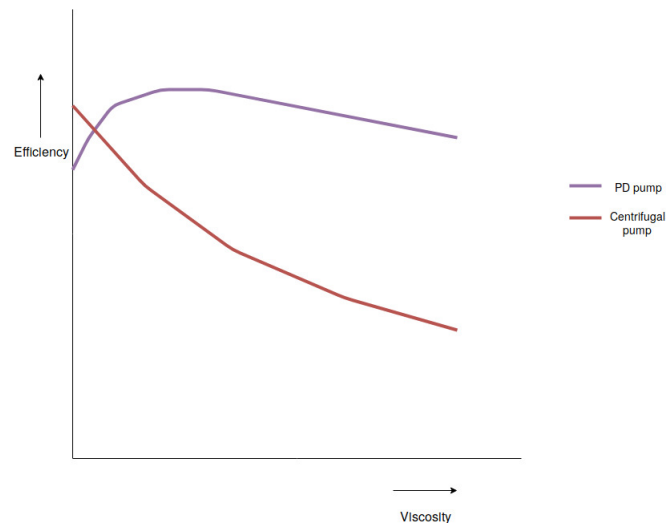
Figure 1.7: Efficiency as a function of Viscosity for centrifugal and positive displacement pumps [20]

Table 1.6 presents an overview of the comparison centrifugal and positive displacement pumps.

Table 1.6: Differences between Centrifugal pumps and Positive Displacement pumps

Centrifugal Pumps	Positive Displacement Pumps

• Flow Rate depends on pressure
 	
• Provides high flow rate
 	
• Mostly used in series configurations
 	
• Efficiency drops with high viscosity fluids
 	
• Max particle size depends on impeller dimensions (usually max 300mm)
 	
• Operation should be at optimum point of the pump graphs, influenced by decrease of pump life due to:
 	
    – Shaft deflection
 	
    – Cavitation
	• Flow Rate does not depend on pressure
	
	• Provides low flow rate
	
	• Mostly used in parallel configurations
	
	• Efficiency increases with high viscosity fluids
	
	• Max particle size depends on puppet valves (usually about 6mm)
	
	• Operation can be on any point of the pump graphs

1.6. Filter Sizing

Mesh sizes for filters can be utilized up to μm. The sizes are expressed as: mesh x. Where x is the amount of holes per inch of the filter. Table 1.7 shows the options for different filter sizes [41].

Table 1.7: Different mesh sizes for particle size filtering

US mesh	Microns	Inches	Millimeters
18	1000	0.0394	1.000
20	841	0.0331	0.841
25	707	0.028	0.707
30	595	0.0232	0.595
35	500	0.0197	0.500
40	400	0.0165	0.400
45	354	0.0138	0.354
50	297	0.0117	0.297
60	250	0.0098	0.250
70	210	0.0083	0.210
80	177	0.0070	0.177
100	149	0.0059	0.149
120	125	0.0049	0.125
140	105	0.0041	0.105
170	88	0.0035	0.088
200	74	0.0029	0.074
230	63	0.0024	0.063
270	53	0.0021	0.053
325	44	0.0017	0.044
400	37	0.0015	0.037
450	32	0.0013	0.032
500	25	0.0010	0.025
635	20	0.0008	0.020

<div align="right">

2

</div>

<div align="right">

Concepts

</div>

2.1. Introduction

To provide a solution for the recovery of the Atlantis II metalliferous soil, requirements, design criteria and assumptions were made, which the design needs to comply with:

2.1.1. Requirements

- A long pipeline (146 km) from the Atlantis II field to the shore of Jeddah is used to transport the slurry
- The discharge pipeline will be installed by an existing Allseas pipelay vessel
- The system shall be designed to extract slurry from a water depth of 2200m
- The system shall be able to extract slurry from the whole project area (6km by 10km)
- The flow regime will be chosen, such that the pipeline does not clog, while at the same time the most economical transport of the slurry is pursued

2.1.2. Design Criteria

- Depletion time for the field is set to 25 years
- The system should be able to deal with particles with maximum size of 20 mm
    - If the option of filtering is chosen, the filtering will not obstruct further flow requirements
- Pumps will be used to provide the pressure required to transport the slurry
    - A pump selection will be made between centrifugal pumps and positive displacement pumps
- Anhydrite layers will not be designed for and will be left out of the problem
- The design needs to be able to suck soil of various strengths
- The design needs to be able to influence the dilution of the slurry

2.1.3. Assumptions

- The fluid is incompressible
- Thixotropic behaviour during flow is not considered as it has a positive effect on the pressure required and thus the energy consumption

After the requirements, design criteria and assumptions, different sub-systems were identified and various solutions were proposed for every system. These sub-systems can be divided into the following sub-groups:

- Systems related to transport of the mixture through the pipeline
- End of the transport line position and maneuverability
- Soil activation and suction system

A morphological overview was created which shows the concepts for every sub-system. Different final concepts were composed and compared based on success criteria and an MCA. The chosen systems for each sub-system are shown in the morphological overview, which shows the total final design.

2.2. Sub-Systems

The different identified sub-systems are shown in figure 2.1. With their locations and sub-groups shown, purple shows transport, green shows transport line location and red shows sub-systems for the suction hose.
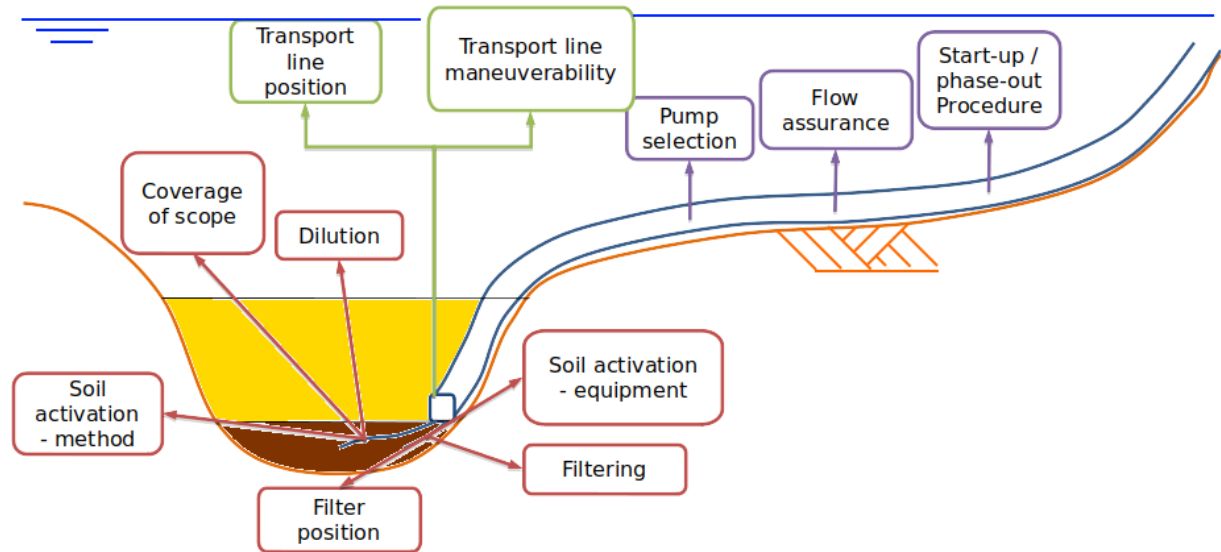
Figure 2.1: Sub-systems locations

2.2.1. Pump Selection

Pumps will be selected for the concept. The proposed pumps are centrifugal pumps and positive displacement pumps. More information about this comparison can be found in chapter 1.

2.2.2. Soil activation method

This sub-system describes the way the soil will be activated, combinations of the proposed sub-systems can be used. Overall cutting will be used for hard layers. Jetting is useful as it can also be utilized as dilution mechanism. Stirring is used to activate the very soft layers, to get the sediment to flow easier.

2.2.3. Dilution

To counteract the salt precipitation and transport lower concentrations with lower power requirement, dilution will be utilized. Jetting functioning as soil activation, can additionally be used to dilute the sediments for transport. A hose to the seawater can be used to simple add regular seawater to the mixture, whereas a hose to the brine can be used to add brine (not fully saturated) to the mixture to dilute it. The final option is to use brine from the location to dilute the mixture, where no hose will be required.

2.2.4. Start-up/Phase-out procedure

As the mixture exhibits thixotropic behaviour, which means an increase in yield strength after a period of rest, the power required to start up the system is higher than when the system is operational. To counteract this phenomenon, either extra power needs to be installed, or the pipeline needs to be flushed before start-up.

2.2.5. Pipeline Extension

This sub-system determines how the concept is able to get to various parts of the mud field.

2.2.6. Flow Regime

The flow regime determines what kind of flow exists in the pipe, related to the size of the particles and velocity of the flow.

2.2.7. Transport line vertical position

This sub-system shows the vertical location of the transport line, if it stops above the brine layer, or the mud layer, the rest of the distance will be covered by a flexible hose with an ROV.

2.2.8. Transport line horizontal position

This sub-system shows if the transport line is moved around, to cover the area of the field, and if so, how it is put into motion. Thrusters attached to the pipeline end can move it around, once it is buoyant. Winches attached to the pipeline end can also move it around, once it is buoyant, which are connected to anchors installed on the far ends of the field.

2.2.9. Suction point mobility

This sub-system shows how the suction point maneuvers over the entire scope of the field.

- **pipeline activation**
  Smaller, extra pipelines of certain raster shapes will be installed with soil activating elements. These pipelines will transport the mixture to the main transport line.
- **floating hose equipment**
  The transport line is buoyant above the field and with flexible hoses and soil activating elements the field will be exploited.
- **Floating equipment**
  Floating platforms are attached to the main line by flexible hoses and an umbilical, activate the soil and feed it to the main line.
- **Surface Trawler**
  This equipment drives over the mud layer with buoyancy attached and activates the soil behind it like a trawler. It is connected by a flexible hose to the main line.

2.2.10. Filtering

The effect of what filtering will be applied, is shown in this sub-system.

2.2.11. Filtering Position

This sub-system shows if filtering is applied at the start of the transport line, somewhere inside it, on multiple locations in the line or outside the line by separate units (hydro cyclones). It will be hard/impossible to filter out particles in the sizes μm by hydrocyclones, while also desiring transport of particles in the order μm.

2.3. Morphological Overview

Figure 2.2 and 2.3 show the morphological overview of all components, including the sub-systems. Table 2.1 shows the morphological overview in a more compact table format. In total there are 82944 combinations if for the sub-systems one choice is picked. If combinations are made, this amount goes up even further. There are some combinations which go hand-in-hand and others which are not viable, for example:

- If soil activation is done by jetting, it is easy to also provide the dilution by jetting
- If the choice is made to filter particles which are not of interest, it makes sense to install filters on multiple locations (different sizes of particles to filter) or outside the pipeline (hydrocyclone) and to keep a turbulent flow regime, to have the mixture be homogeneous.
- Using positive displacement pumps, the choice for installing extra power in a parallel configuration to combat the thixotropic behaviour is an option, for centrifugal pumps, which need to be installed in series and are used for high flow rates, this is a bad option. Using centrifugal pumps the pipeline will be flushed with water, which is a relatively fast process, due to the high flow rate available.
- If the choice for jetting is not made, then a hose to the seawater is necessary, not only to counter the salt precipitation, but also to provide the lowest power consumption possible.
- For any of the options containing a movable, buoyant transport line, the vertical position of the pipeline will be near the mud layer. Also, a flexible suction hose from atop the brine layer is not very practical.

Based on the morphological overview, different concepts were formed out of every sub-system. The four most promising concepts were evaluated by success criteria and a Multi Criteria Analysis. The four different concepts are:

- Flexible suction hose
- Floating platform

- Expandable pipe
- Horizontal trawler

Figure 2.2: Morphological overview part 1

Transport line vertical position	to the mud layer	to the brine layer

Transport line horizontal position	Stationary	Floating, moved by winches	Floating, moved by thrusters

Suction point mobility	Pipeline activation	Floating hose equipment	Floating equipment	Surface crawler

Filtering	No filtering	Filter particles that can not be transported	Filter particles that are not of interest

Filtering position	Front end of the suction pipe	Inside the suction pipe	Multiple locations in the suction pipe	Hydro cyclone

Figure 2.3: Morphological overview part 2

Table 2.1: Morphological overview table

Pumps	Positive Displacement Pumps			Centrifugal Pumps		
Soil activation - method	Jetting		Cutting		Stirring	
Dilution	Jetting	Hose to sea water		Hose to brine	Brine from location	
Start up / Phase out procedure	Flush Pipeline			Install extra pumping power		
Coverage of scope	Moveable suction pipes			Expandable system		
Flow assurance	Laminar flow		Transition region		Turbulent flow	
Transport line **vertical** position	On the sea bed to the mud layer			On the sea bed to the brine layer		
Transport line **horizontal** position	Stationary		Floating, moved by winches attached to anchors		Floating, moved by thrusters	
Suction point mobility	Pipeline activation	Floating hose equipment		Floating equipment		Surface crawler
Filtering	No filtering	Filter particles that can not be transported		Filter particles that are not of interest		
Filter position	Front end of the suction pipe	Inside the suction pipe		Multiple locations in the suction pipe		Hydro cyclone

These concepts were rated against various criteria in a Multi Criteria Analysis (MCA).
For this MCA, first the different criteria were weighted against each other, to determine which criteria are most important and which are of less importance. This weight will be used as multiplication to the score given to that concept on that criteria. In the end, each concept will have a final score, based on all their score on all criteria and the relevant weighting factor.
This gives an indication of what concept would be most feasible, however, no conclusions have to be drawn regarding this outcome.

2.4. Concepts
Different concepts were formed, the four most promising ones were compared and are shown in figures 2.4, 2.5, 2.6 and 2.7. In appendix E the specific morphological overviews are shown, for the four concepts.

2.4.1. Flexible suction hose
In this concept the transport pipeline is kept afloat in the brine layer by buoyancy elements and is moved in horizontal position by winches installed to the pipeline and anchors installed on the seabed at the same depth as the pipeline end.
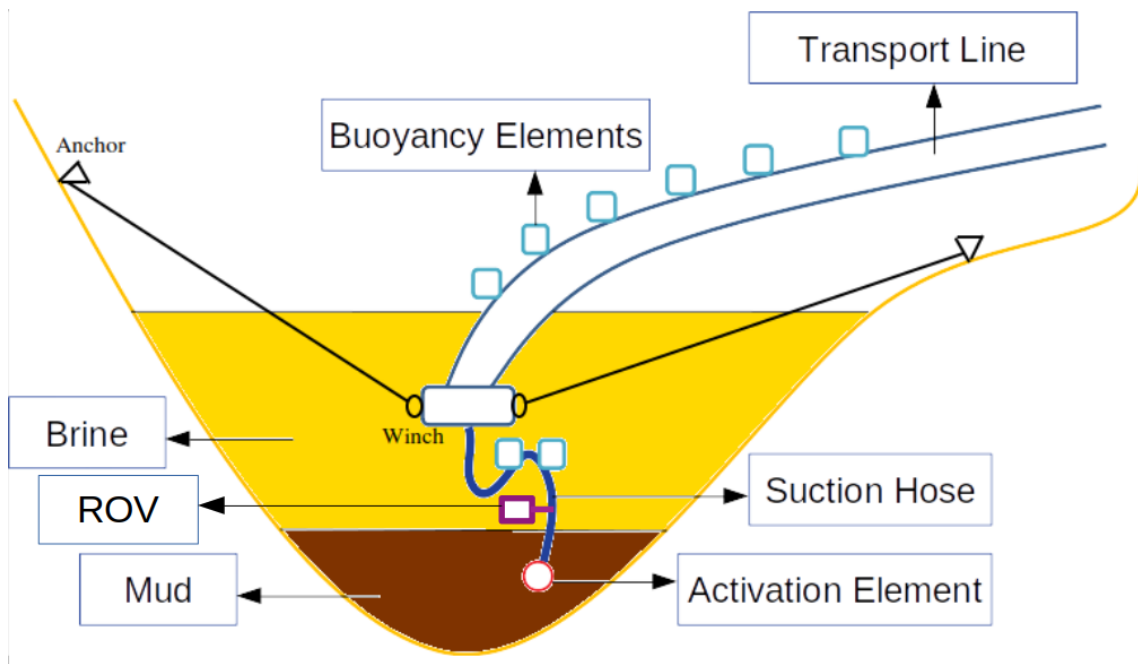
Figure 2.4: Concept - Flexible hose

2.4.2. Floating platform

In this concept the transport line is kept at a constant position and the floating platforms, connected to the pipeline end, take care of the activation and suction of the soil.
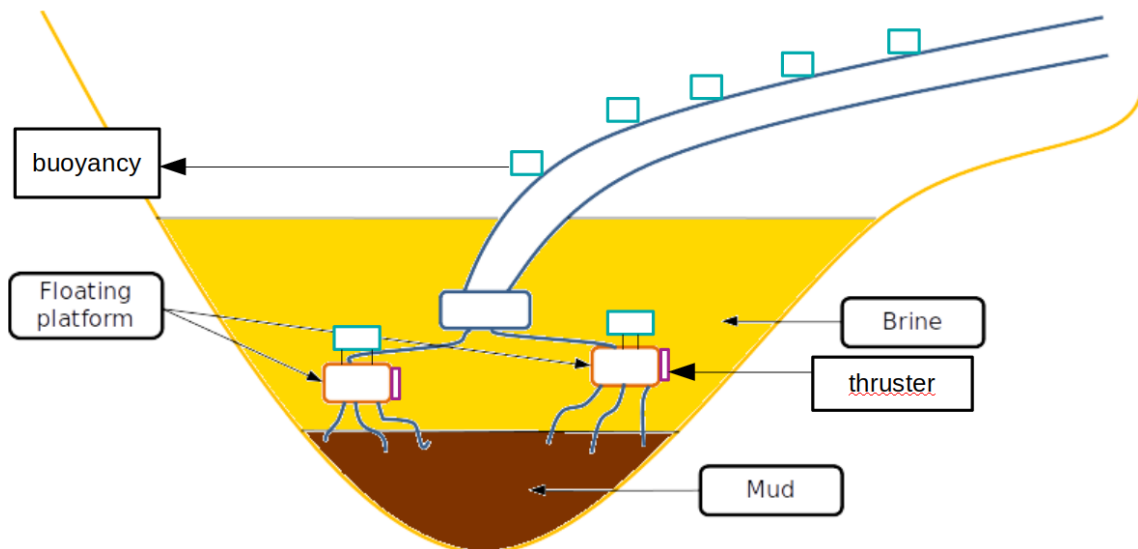
Figure 2.5: Concept - Floating Platform

2.4.3. Expandable pipe

This concept focuses on the point that a pipe with activating elements is deployed on the sea bed. This pipe is connected to the main transport line. Once a certain depth/area has been dredged, the pipeline can be expanded or relayed to another position.

There are limited moving parts in this concept, which can make it an interesting choice.
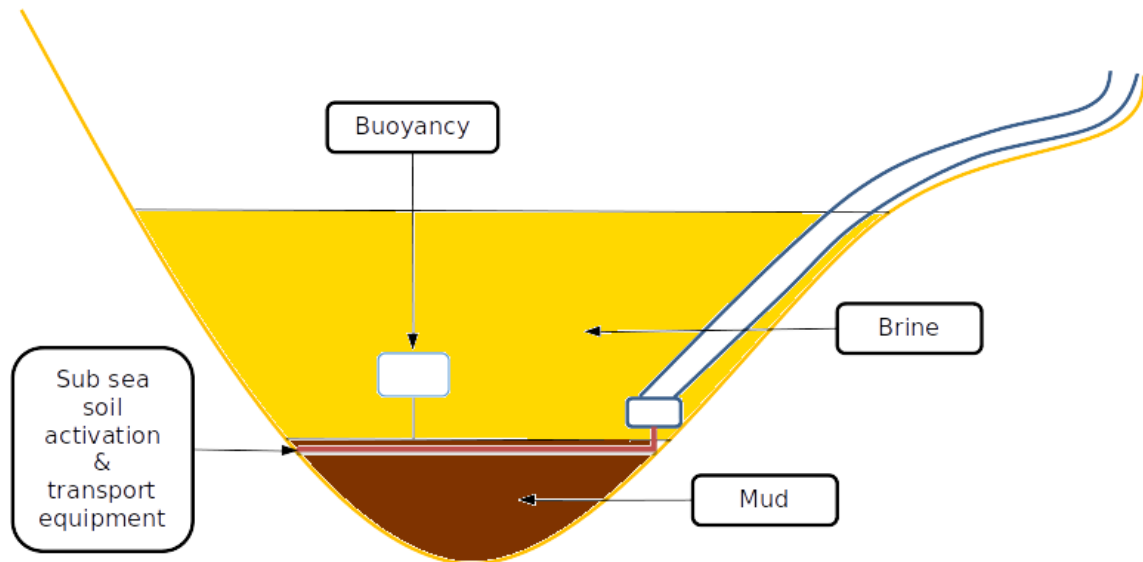
Figure 2.6: Concept - Expandable Pipe

2.4.4. Horizontal trawler

For this concept a trawler is used near the sea floor. This trawler moves in horizontal direction and is connected to the transport line by a flexible hose. The trawler provides activation of the soil as well as suction.
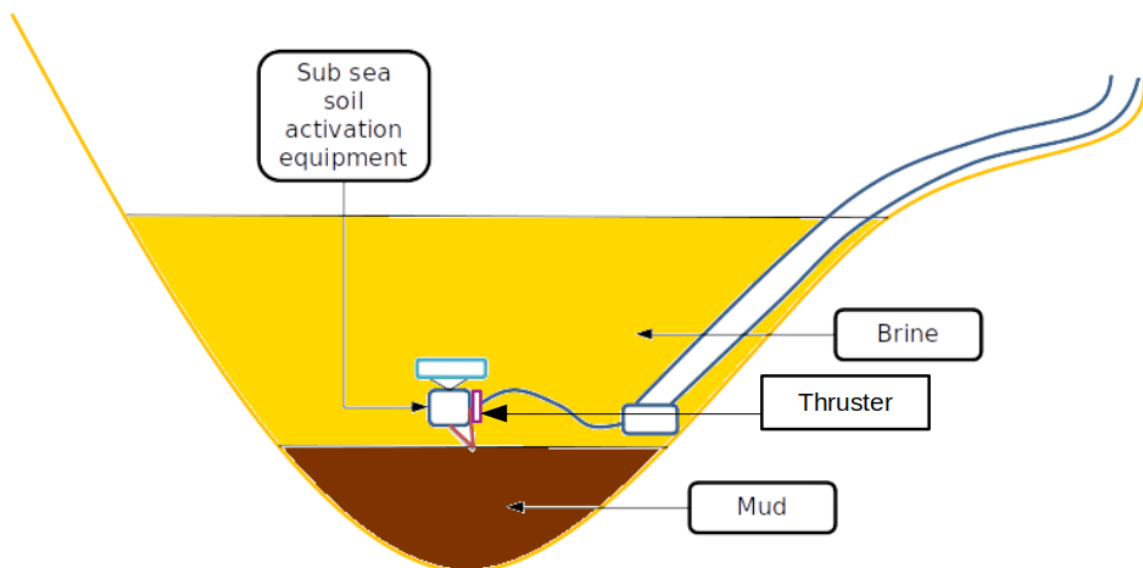
Figure 2.7: Concept - Horizontal Trawler

2.5. Multi Criteria Analysis

Based on the different concepts, a Multi Criteria Analysis was formed to score the concepts on different criteria, which will have their own weighting factor. The criteria are:

- Power Consumption
- No Clogging
- Maintenance
- Soil Activation Efficiency
- Durability
- Simplicity
- Maneuverability

These criteria are compared to one another to affirm which criteria are most important for the provided rating. The table works from left to right. A 1 in the cell means the criteria on the left, in the red column, is more important than the criterium in the red row at the top. A 0.5 means the criteria are valued evenly.

Table 2.2: Weighting factors of the Multi Criteria Analysis

	Power Consumption	No Clogging	Maintenance	Soil Activation Effiency	Durability	Simplicity	Maneuverability	Total	Weighting factor
Power Consumption		0.5	1	1	1	1	1	5.5	1.92
No Clogging	0.5		1	1	1	1	1	5.5	1.92
Maintenance	0	0		0	0	0	0	0	1.00
Soil Activation Effiency	0	0	1		1	0	1	3	1.50
Durability	0	0	1	0		0	0	1	1.17
Simplicity	0	0	1	1	1		1	4	1.67
Maneuverability	0	0	1	0	1	0		2	1.33

With the weighing factors per criterium known, the weighted total of the concepts can be determined. The weighted total is score of the concept times the weighting factor, determined for the criterium.
Per criterium the various concepts are evaluated against each other, a 1 means the concept on the left, in the red column, is rated higher than the concept shown on top in the red row.

Table 2.3: Weighted totals per criterium of the Multi Criteria Analysis

MCA criteria 1: Power Consumption

	Concept 1: Flexible Suction Hose	Concept 2: Floating Platform	Concept 3: Expandable Pipe	Concept 4: Horizontal Trawler	Total	Weighting Factor	Weighted Total
Concept 1: Flexible Suction Hose		1	1	1	3	1.92	5.75
Concept 2: Floating Platform	0		0	0.5	0.5	1.92	0.96
Concept 3: Expandable Pipe	0	1		1	2	1.92	3.83
Concept 4: Horizontal Trawler	0	0.5	0		0.5	1.92	0.96

MCA criteria 2: No Clogging

	Concept 1: Flexible Suction Hose	Concept 2: Floating Platform	Concept 3: Expandable Pipe	Concept 4: Horizontal Trawler	Total	Weighting Factor	Weighted Total
Concept 1: Flexible Suction Hose		0	1	0	1	1.92	1.92
Concept 2: Floating Platform	1		1	0.5	2.5	1.92	4.79
Concept 3: Expandable Pipe	0	0		0	0	1.92	0.00
Concept 4: Horizontal Trawler	1	0.5	1		2.5	1.92	4.79

MCA criteria 3: Maintenance

	Concept 1: Flexible Suction Hose	Concept 2: Floating Platform	Concept 3: Expandable Pipe	Concept 4: Horizontal Trawler	Total	Weighting Factor	Weighted Total
Concept 1: Flexible Suction Hose		1	1	1	3	1.00	3.00
Concept 2: Floating Platform	0		0.5	0.5	1	1.00	1.00
Concept 3: Expandable Pipe	0	0.5		0.5	1	1.00	1.00
Concept 4: Horizontal Trawler	0	0.5	0.5		1	1.00	1.00

MCA criteria 4: Soil Activation Effiency

	Concept 1: Flexible Suction Hose	Concept 2: Floating Platform	Concept 3: Expandable Pipe	Concept 4: Horizontal Trawler	Total	Weighting Factor	Weighted Total
Concept 1: Flexible Suction Hose		0.5	1	0.5	2	1.50	3.00
Concept 2: Floating Platform	0.5		1	0.5	2	1.50	3.00
Concept 3: Expandable Pipe	0	0		0	0	1.50	0.00
Concept 4: Horizontal Trawler	0.5	0.5	1		2	1.50	3.00

MCA criteria 5: Durability

	Concept 1: Flexible Suction Hose	Concept 2: Floating Platform	Concept 3: Expandable Pipe	Concept 4: Horizontal Trawler	Total	Weighting Factor	Weighted Total
Concept 1: Flexible Suction Hose		1	0.5	1	2.5	1.17	2.92
Concept 2: Floating Platform	0		0	0.5	0.5	1.17	0.58
Concept 3: Expandable Pipe	0.5	1		1	2.5	1.17	2.92
Concept 4: Horizontal Trawler	0	0.5	0		0.5	1.17	0.58

MCA criteria 6: Simplicity

	Concept 1: Flexible Suction Hose	Concept 2: Floating Platform	Concept 3: Expandable Pipe	Concept 4: Horizontal Trawler	Total	Weighting Factor	Weighted Total
Concept 1: Flexible Suction Hose		1	1	1	3	1.67	5.00
Concept 2: Floating Platform	0		0	0.5	0.5	1.67	0.83
Concept 3: Expandable Pipe	0	1		1	2	1.67	3.33
Concept 4: Horizontal Trawler	0	0.5	0		0.5	1.67	0.83

MCA criteria 7: Maneuverability

	Concept 1: Flexible Suction Hose	Concept 2: Floating Platform	Concept 3: Expandable Pipe	Concept 4: Horizontal Trawler	Total	Weighting Factor	Weighted Total
Concept 1: Flexible Suction Hose		0	1	0	1	1.33	1.33
Concept 2: Floating Platform	1		1	0.5	2.5	1.33	3.33
Concept 3: Expandable Pipe	0	0		0	0	1.33	0.00
Concept 4: Horizontal Trawler	1	0.5	1		2.5	1.33	3.33

Now the weighted totals are known for the various concepts based on the different criteria and the total scores can be determined.

Table 2.4: Multi Criteria Analysis - Concept scores

	Concept 1: Flexible Suction Hose	Concept 2: Floating Platform	Concept 3: Expandable Pipe	Concept 4: Horizontal Trawler
Power Consumption	5.75	0.96	3.83	0.96
No Clogging	1.92	4.79	0.00	4.79
Maintenance	3.00	1.00	1.00	1.00
Soil Activation Effiency	3.00	3.00	0.00	3.00
Durability	2.92	0.58	2.92	0.58
Simplicity	5.00	0.83	3.33	0.83
Maneuverability	1.33	3.33	0.00	3.33
TOTAL	22.92	14.50	11.08	14.50

Based on the MCA, the concept with the highest score is the flexible suction hose

2.6. Chosen Concept

Based on the MCA, the chosen concept is the flexible suction hose. For this concept a single suction hose will be moved flexibly by an ROV and the transport line's position horizontally will be guaranteed by winches, while the vertical position will be attended to by buoyancy modules. At the end of the flexible hose there will be a soil activation device, to loosen the soil and prepare it for transport by the transport line.
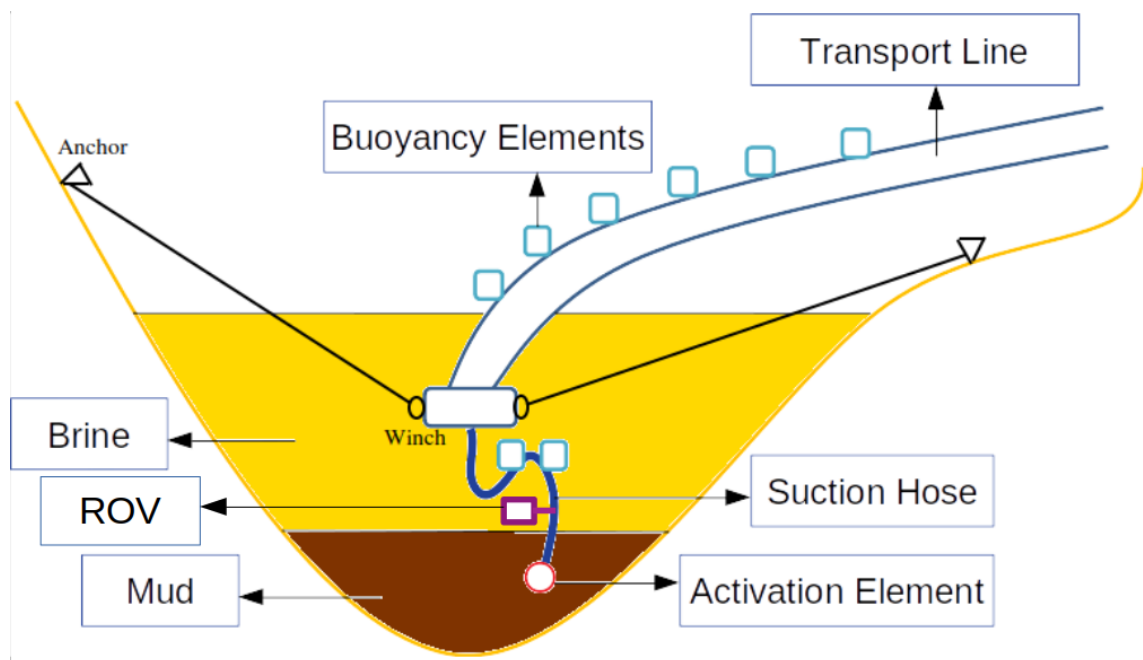
Figure 2.8: Concept - Flexible hose

Bibliography

[1] Nico Augustin, Mark Schmidt, Colin Devey, Benjamin Kürten & 42 others (December 2014) *The Jeddah Transect Project: Extensive mapping of the Red Sea Rift*
Projects: Geomorphology, volcanism, hydrothermalism and salt kinematics of the Red Sea Rift, Jeddah Transect - a bi-lateral project between the King Abdulaziz University, KSA, and Helmholz Center of Ocean Research, GER

[2] Erik A. Toorman. *Thixotropy model for cohesive sediment suspensions*
Rheologica Acta, Vol. 36, No. 1 (1997) ©Steinkopff Verlag 1997

[3] Moore F. (1959) *The rheology of ceramic slips and bodies*
Trans Brit Ceramic Soc 58:470-494

[4] Groundforce, specialist construction solutions. *Soil Description Chart*
Description generally in accordance with BS 5930:1999.

[5] Josh Smith, C. Modenesi, M. Salca-Ramirez, G. Castro, C. Santamarina, 09-09-2018 *Metalliferous Sediments in the Red Sea: From Resource to Reserve*
UMC 2018 - EGEL KAUST

[6] John R. Rumble, ed. (2018) *CRC Handbook of Chemistry and Physics (99th ed.)*
Boca Raton, FL: CRC Press. ISBN 978-1138561632.

[7] *- Dredge Pumps & Slurry Transport, Lecture Notes: Intermezzo I p.6*

[8] *- Dredge Pumps & Slurry Transport, Lecture Notes: Chapter 4 - Matousek*

[9] Dr. P.R. Williams *Rheometry for non-Newtonian fluids*
Department of Chemical and Biological Process Engineering, University of Wales Swansea

[10] L.W. van den Broecke (2018). *A Study into the Characteristics of the Cohesion-Adhesion Relation and its Effects on Cutting Processes in Dredging Engineering*
Master Thesis

[11] T. Horst (2019) *The influence of flocculation on the development of a sediment plume*
Master Thesis

[12] Yotaro Hatamura & Kenji Chijiiwa. *Analysis of the mechanism of soil cutting: 1st Report. Cutting patterns of soils*
January 1975, DOI: 10.1299/jsme1958.18.619

[13] Yotaro Hatamura & Kenji Chijiiwa. *Analysis of the mechanism of soil cutting: 2nd Report. Deformation and Internal Stress of soil in Cutting*
May 1976 DOI: 10.1299/jsme1958.19.555

[14] Yotaro Hatamura & Kenji Chijiiwa. *Analysis of the mechanism of soil cutting: 4th Report. Properties of Soils Related to Cutting*
January 1977 DOI: 10.1299/jsme1958.20.130

[15] Yotaro Hatamura & Kenji Chijiiwa. *Analysis of the mechanism of soil cutting: 5th Report. Cutting Theories of Soils*
January 1976 DOI: 10.1299/kikai1938.42.2258

[16] Dr. ir. Sape A. Miedema. *New Developments of Cutting Theories With Respect To Dredging the Cutting of Clay*
June 1992, Conference: World Dredging Conference XIII. At: Bombay, India.

[17] Dr. ir. Sape A. Miedema. *The Delft Sand, Clay & Rock cutting model*
© 2014-2015 Dr.ir. S.A. Miedema and IOS Press. All rights reserved. Preliminary edition: ISBN Book: 978-94-6186-249-5

[18] Churchill S.W. (1977). *Friction-factor equation spans all fluid-flow regimes*
Chemical Engineering, 84(24), 91-2.

[19] Matousek, V. (1997). *Flow Mechanism of Sand-Water Mixtures in Pipelines*
Delft University Press.

[20] 1998 Viking Pump, Inc. *When to use a positive displacement pump*
Retrieved from:
www.pumpschool.com

[21] Michael Smith engineers ltd., The UK's Leading Pump Specialist. *Useful information on positive displacement pumps*
Retreived from:
https://www.michael-smith-engineers.co.uk/resources/useful-info/positive-displacement-pumps

[22] © 2003, 2008 Randall W. Whitesides, CPE, PE *Practical Considerations in Pump Suction Arrangements*

[23] ASTM D4943-18, *Standard Test Method for Shrinkage Factors of Cohesive Soils by the Water Submersion Method*
ASTM International, West Conshohocken, PA, 2018, www.astm.org

[24] Dr. ir. Sape A. Miedema. *Slurry Transport - Fundamentals, A Historical Overview & The Delft Head Loss & Limit Velocity Framework*
© 2013-2019 Dr.ir. S.A. Miedema. 2nd Edition: ISBN EBook: 978-94-6366-141-6. Licensed under CC BY-NC-SA 4.0

[25] Junghee Park, J. Carlos Santamarina. *Revised soil classification system RSCS*
Earth Science and Engineering Department, King Abdullah University of Science and Technology (KAUST), Thuwal 23955-6900, Saudi Arabia, junghee.park@kaust.edu.sa

[26] www.metalary.com

[27] www.infomine.com

[28] Al Ukayli, M., Guney, M. Al Mahhoun, M. Born, R. (1981) *Geostatistical Evaluation of Metal Reserves of the Atlantis II Deep, Red Sea, Final Report, Metal Reserve Evaluation Volume I - V.*
Research Institute University of Petroleum & Minerals, Dhahran, S.A.

[29] Bertram, C., Kratschell, A., O'Brian, K., Brackmann, W., Proelss, A., Rehdanz, K., (2011) *Metalliferous Sediments in the Atlantis II Deep - Assessing the Geological and Economic Resource Potential and Legal Constraints.*
Kiel Working Papers 1688, Kiel Institute for the World Economy

[30] Guney, M., Nawab, Z., Marhoun, M.A., (1984) *Atlantis II Deep's Metal Reserves and their Evaluation*
Offshore Technology Conference 1984

[31] Robert J. Visintainer, P.E., George S. McCall II, P.E., Jogn M. Furlan, Ph.D., Travis E. Basinger *Dead Sea Works Salt Recovery Project Slurry Testing - Phase 1*
18 September 2014 Rev. A GIW Hydraulic Laboratory
GIW Industries, Inc. - A KSB Company
5000 Wrightsboro Rd., Grovetown, Georgia, USA

[32] Jorge Parrondo, Sandra Velarde-Suárez, Carlos Santolaria. *Development of a predictive maintenance system for a centrifugal pump*
(1998) Journal of Quality in Maintenance Engineering. 4. 198-211. 10.1108/13552519810223490.

[33] Weir Slurry Division, A division of WEIR GROUP PLC. *Slurry Pumping Manual, A technical application guide for users of centrifugal slurry pumps and slurry pumping systems*
First edition, © 2002 Warman International LTD.

[34] P.K. Swamee and N. Aggerwall (2011) *Explicit equations for laminar flow of Bingham plastic fluids*
Journal of Petroleum Science and Engineering

[35] A. Casagrande (1932) *Research on the Atterberg limit of soils*
Public Roads 12(3), pp. 121-30 and 136

[36] H. Darcy (1857) *Recherches experimentales relatives au mouvement de l'eau dans le tuyaux*
Mallet-Bachelier, Paris. 268 p. (French)

[37] J. Weisbach (1845) *Lehrbuch der Ingenieur- und Maschinen-Mechanik, Vol. 1: Theoretische Mechanik*
Vieweg und Sohn, Braunschweig. 535 p. (German)

[38] E. Buckingham (1921) *On plastic flow through capillary tubes.*
ASTM proceedings. 21: 1154-1156

[39] R. Darby & J. Melson. (1981) *How to predict the friction for flow of Bingham plastics*
Chemical Engineering 28. 59-61.

[40] A.B. Metzner and J.C. Reed. (1955) *Flow of non-Newtonian fluids - correlation of the laminar, transition and turbulent-flow regions.*
AIChE J. 1(4):434-40

[41] ISM Industrial Specialties Mfg. and IS MED Specialties ISO 9001:2008 Certified Companies *Mesh and Microns Conversion Chart and Information E-book from ISM*
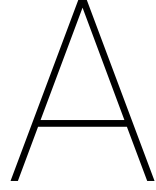
Rabinowitsch-Mooney

The Rabinowitsch-Mooney [9] equation gives an expression for the shear rate in a pipeline for a non-Newtonian fluid as a function of beam - r of the pipe.

$$dQ = 2\pi r dr \cdot V_x \tag{A.1}$$

Integrating by parts gives

$$Q = 2\pi \left(\left[\frac{r^2 v_x}{2} \right]_0^{r_i} + \int_0^{r_i} \frac{r^2}{2} \left(\frac{-dv_x}{dr} \right) dr \right) \tag{A.2}$$

For a no-slip condition, the first term vanishes from equation, leading to:

$$Q = \pi \int_0^R r^2 (-\dot{\gamma}) dr \tag{A.3}$$

If the fluid is time-independant and homogeneous, the shear stress is a function of ONLY the shear rate:

$\tau_{rx} = f(\dot{\gamma})$ and inversely: $\dot{\gamma} = f(\tau_{rx})$

$$\frac{\tau_{rx}}{\tau_w} = \frac{r}{R} \tag{A.4}$$

Using equation $A.4$ to reformulate r, the following can be obtained:

$$Q = \pi \int_0^{\tau_w} \frac{\tau^2 R^2}{\tau_w^2} (-\dot{\gamma}) \frac{\tau_i}{\tau_w} d\tau = \frac{\tau R^3}{\tau_w^3} \int_0^{\tau_w} \tau^2 (-\dot{\gamma}) d\tau \tag{A.5}$$

Where $\dot{\gamma}$ is interpreted as: $f(\tau)$ and not $f(\tau, r)$

Equation: $A.5$ can be written in terms of flow characteristics

$$\frac{8u}{D} = \frac{4Q}{\pi R^3} = \frac{4}{\tau_w^3} \int_0^{\tau_w} \tau^2 (-\dot{\gamma}) d\tau \tag{A.6}$$

Equation $A.6$ is multiplied by τ_w^3 and subsequently differentiated with respect to τ_w.
Afterwards, equation $A.7$ is obtained.

$$3\tau_w^2 \frac{8u}{D} + \tau_w^3 \frac{d(\frac{8u}{D})}{d\tau_w} = 4\tau_w^2 (-\dot{\gamma})_w \tag{A.7}$$

Equation $A.7$ can be rearranged to obtain equation $A.8$.

$$-\dot{\gamma}_w = \frac{8u}{D} \left[\frac{3}{4} + \frac{1}{4} \frac{\tau_w}{\frac{8u}{D}} \frac{d(\frac{8u}{D})}{d\tau_w} \right] \tag{A.8}$$

With $\dfrac{dx}{x} = d\ln x$ gives for equation A.8:

$$-\dot{\gamma}_w = \frac{8u}{D} \left[\frac{3}{4} + \frac{1}{4} \frac{d\ln\frac{8u}{D}}{d\ln\tau_w} \right] \tag{A.9}$$

Wall shear rate for Newtonian fluids is defined as: $= \dfrac{-8u}{D}$

so shear rate can be expressed in shear rate for a Newtonian fluid.

$$\dot{\gamma}_w = \dot{\gamma}_{wN}\left[\frac{3}{4} + \frac{1}{4}\frac{d\ln\frac{8u}{D}}{d\ln\tau_w}\right] \tag{A.10}$$

In equation $A.10$, $\left[\frac{3}{4} + \frac{1}{4}\frac{d\ln\frac{8u}{D}}{d\ln\tau_w}\right]$ is called *the correction factor*.

Equation A.10 shows the Rabinowitsch-Mooney equation. It shows that the wall shear rate of a non-Newtonian fluid can be calculated from the value of a Newtonian fluid with the same flow rate.
A measurement and calculation procedure will be listed in A.

1. Measure Q at various values of $\frac{\Delta P_f}{L}$, preferably eliminating end effects.

2. Calculate τ_w from pressure drop measurements and the corresponding values of the flow characteristic: $\frac{8u}{D} = \frac{4Q}{\pi R^3}$

3. Plot $\ln\frac{8u}{D}$ against $\ln\tau_w$ and measure gradient at various points on the curve. Alternatively the gradient from the differences between the successive values of these quantities.

4. Calculate the true wall shear rate from equation A.9 or A.10 with the derivative determined in step 3. In general, the plot of $\ln\frac{8u}{D}$ against $\ln\tau_w$ will not be a straight line and the gradient must be determined.

<div align="right">

B

</div>

Practical determination of the pressure gradient

Depending on slurry-, pipeline- and pressure parameters the desired regime for transport is obtained. Based on these parameters the pressure gradient can be determined. There are two different ways to do this and both will be explained:

1. *Flow study*

2. *Rheometer*

- **Flow study**

    1. Estimate pipe diameter based on project lifetime.

    2. Build/Find a loop test facility with test sections in the estimated pipe size range.

    3. Create/Obtain a large enough representative sample of the solids material to be transported.

    4. Create/Obtain a large enough representative sample of the suspending liquid.

    5. Determine solids content of the slurry to be transported.

    6. Prepare a slurry sample with higher solid content than the estimated/calculated amount.

    7. Measure the pressure gradient ($\frac{\Delta P}{L}$) over a large range of volumetric flow rates (Q) in the loop test facility.

    8. Dilute the slurry with suspending liquid at least 2 times to obtain pipe flow curves at various solid contents.

    9. Determine hydraulic gradient for different pipe diameters and solid contents by interpolating between results.

- **Rheometer**

    1. Obtain a standard rheometer (capillary or concentric cylinder)

    2. Create/Obtain a small representative sample of the solids material to be transported.

    3. Create/Obtain a large enough representative sample of the suspending liquid.

    4. Create 3 slurry samples which span the expected solids content range.

    5. Measure the shear stress against the shear rate in the rheometer.

    6. Fit the shear stress-shear rate relation of every sample to a constitutive equation, like in table 1.3.
    Bingham fluid:
    $\tau = \tau_B + \eta_B \dot{\gamma}$

7. Fit a semi-empirical model to the rheological constants at the different solid contents. For a Bingham plastic, which is a non-Newtonian fluid with a yield stress and linear relation between viscosity and shear rate, the following physical relation can be used:

$$\tau_B = C_0\phi^{C_1} \text{ and } \eta_B = \mu \cdot exp(C_2\phi)$$

Where μ is the viscosity of the carrier fluid and $C_0, C_1 and C_2$ are determined from the Bingham fit to the data.

8. Use the physical relationships to estimate the rheological behaviour for all values in the test range:
$\tau \approx C_0\phi^{C_1} + \mu \cdot exp(C_2\phi)\dot{\gamma}$

9. Use solid and liquid density to calculate the slurry density:
$\rho = \phi\rho_s + (1-\phi)\rho_l$

10. Determine the laminar flow velocity (V_L) as a function of the pressure gradient, using the Buckingham design equation:
$V_L = \frac{D\tau_w}{8\eta_B}(1 - \frac{4}{3}Z + \frac{1}{3}Z^4)$
Where:
$Z = \frac{\tau_B}{\tau_w}$ and $\tau_w = \frac{\Delta P}{L}\frac{D}{4}$

11. Determine the turbulent flow velocity (V_T) as a function of the pressure gradient using Wilson-Thomas:
$V_T = 2.5u \cdot \ln(\frac{\rho Du^*}{\eta_B}) + 2.5u \cdot \ln(\frac{1-Z}{1+Z}) + u \cdot Z(14.1 + 1.25Z)$
Where:
$u^* = \sqrt{\frac{\tau_w}{\rho}}$

12. Make use of or create a spreadsheet to generate the pressure gradient against flow curves for different pipe diameters and solid contents.

C
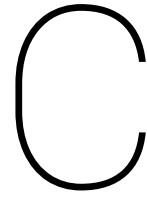
Suction Mouth

C.1. Shape

Different shapes of suction mouths are applicable to different applications.

- **Blocked at the sides**
  This shape can be compared to the Coanda nozzle, when approached analytically. It is currently under investigation to be used for deep sea nodule mining. The water volume which is sucked by the main pipe is constant. Placing the pipe closer to the seabed decreases the area through which the water can flow, therefore increasing its velocity. The water with higher velocity can loosen the nodules from the seabed and transport them through the harvester.
  The limit deposit velocity can be used as flow velocity for which the nodules are still transported by the water. The highest flow velocity is near the edges of the pipe with the Blocked sides.

- **Upside down diffuser**
  The main upside to an upside down diffuser is that it increases the area over which sediment is captured. This is therefore the reason they are mostly used in combination with cutter suction dredges. These dredges cause for a lot of spilling due to centrifugal forces, the upside down dispenser has the largest area over which these sediments can still be captured.

- **Straight shape**
  This shape can be used to erode non-cohesive soils. Near the pipeline ends the flow compacts, leading to an increase in velocity and turbulence. This increase in velocity and turbulence leads to the erosion. It is for this reason straight inlet shapes are used in diamond mining, off the west coast of Africa. The diamonds are entrapped in sandy soils, eroding the sand exposes the diamonds, which can then be sucked up and transported for production.
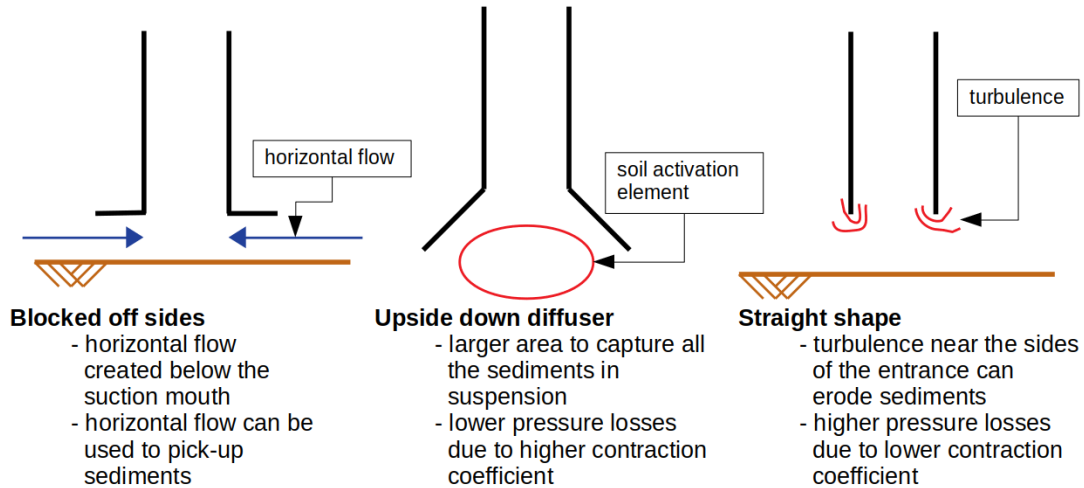
Figure C.1: Three different inlet shapes with their pros and cons

C.2. Pressure Losses

Pressure losses for suction systems can be expressed in formula C.1.

$$\xi \cdot \frac{\rho u^2}{2} \tag{C.1}$$

ξ is called the contraction coefficient. Depending on the shape and extended curvature of the pipe, this value may increase to about three, for very flow-unfriendly shapes.

For short dredging pipelines, which usually operate on high flow velocities ($\pm 7 \frac{m}{s}$), due to needing to be able to transport any sizes of particles, this can lead to very dominant pressure losses. Equation C.2 shows the pressure losses for flow.

$$\lambda \cdot \frac{L}{D} \cdot \frac{\rho u^2}{2} \tag{C.2}$$

A relation can be drawn between the pressure losses due to transport and due to the suction mouth. If we assume a suction mouth with a contraction coefficient of 3, a hydraulic gradient of 0.01 for water pumping and a pipeline with a diameter of one meter, this would lead to pressure loss over the suction mouth being equal to transport over 300 meters of pipeline.

From this relation the conclusion is drawn that for transport in a 146km long pipeline, the shape of the suction mouth is of little influence, for shorter transport lengths however, it can make a big difference.

D

CFD - OpenFOAM

D.1. Introduction

An attempt was made to create a CFD model to provide extra verification of the chosen concept. Verification was required for laminar and turbulent flow regimes, of both Newtonian and non-Newtonian fluids. The chosen concept requires turbulent flow of a non-Newtonian fluid, which is where the simulation verification, by applying the Bingham plastic model, failed. The error for the empirical formula and the results from the CFD simulation were at least 30% which was deemed to large to continue.

Simulating flow in pipeline has shown that it is extremely important for results, to create a mesh which has a constant distribution of cells in the length direction of the pipeline. This is most easily accomplished by a mesh consisting of hexahedrons.
To get the pipeline to be meshed by hexahedrons, it makes sense to create the 1d area element of the pipeline, as a divided disk of five separate elements. With the one in the middle being a square and the outer four having the exact same shapes.
The pipeline model is a pipe with length 1m and diameter 1 cm. The mesh depends on whether a wall function is applied or not.

D.2. Laminar-Turbulent Newtonian-non-Newtonian flow

Four cases will be reviewed:
- laminar, Newtonian
- turbulent, Newtonian
- laminar, non-Newtonian
- turbulent, non-Newtonian

To determine the pressure losses, velocity is determined at the inlet, so that laminar or turbulent regime are guaranteed. Pressure at the outlet is set at 0, so the pressure value at the inlet can be calculated and the pressure losses over slurry transport of the case will be known.
RANS (Reynolds Averaged Navier-Stokes) turbulence modeling was applied for the turbulence models. This is done with either the k-ϵ or k-SS-ω model. Both models give similar results and therefore the k-ϵ model is used, as this is easier to apply.
A wall-function was used to capture viscous effects near the pipeline wall for turbulent flow, instead of using a full resolution approach with very small cell sizes near the wall.

D.2.1. Laminar Newtonian

This is the easiest case to confirm, water will be used as Newtonian fluid. First the Reynolds number is calculated for a laminar case. In this example a pipe of 1m length and diameter of 0.01m. Velocity at the inlet will be set to uniform 0.01, leading for laminar flow to develop a velocity of 0.02 in the middle of the pipe, where the flow is no longer uniform.

This case leads to a Reynolds number of:

$$\text{Re} = \frac{\rho \cdot D \cdot u}{\nu} = \frac{1000 \cdot 0.01 \cdot 0.01}{0.001} = 100$$

Laminar flow occurs for Reynolds numbers < 2100, so this case is well within the laminar regime. Comparing the results of laminar flow of water with the empirical equation gives identical results as the CFD calculation does for the pressure loss.

The following calculations can be made for the laminar regime:

$$\lambda_{dw} = \frac{64}{100} = 0.64$$

$$P = \lambda_{dw} \frac{L}{D} \frac{\rho u^2}{2}$$

$$P = 0.64 \frac{1}{0.01} \frac{1000 * 0.01^2}{2} = 3.2 \text{Pa}$$

See figure D.1 for the end of the CFD calculation, where the normalized pressure difference between inlet (left) and outlet (right) is shown. Multiplying this with the density ($1000 \frac{\text{kg}}{\text{m}^3}$) gives the absolute pressure difference between inlet and outlet, so for transport over the length of the pipeline, this is 3.28 Pa. Which is very close to the empirical solution.
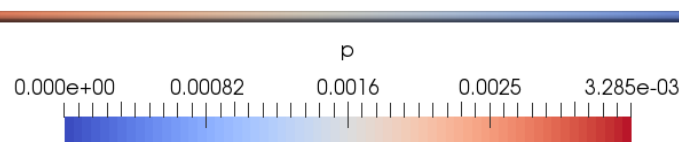
Figure D.1: Laminar Newtonian pipeline flow over 1 meter pipe of 0.01m diameter

D.2.2. Turbulent Newtonian

To capture turbulent effects a RANS (Reynolds Averaged Navier Stokes) turbulence model will be used, this means turbulence effects are statistically averaged over the entire length/area of the mesh, as opposed to LES (Large Eddy Simulation), where local turbulent effects, like eddies will be modeled on scale.

Extra parameters needed are:

- l = turbulent length scale = $0.07 \cdot d_h$
- I = turbulence intensity = $0.16\text{Re}^{\frac{-1}{8}}$
- k = turbulence kinetic energy = $\frac{3}{2}(u_{avg}I)^2$
- C_μ = empirical constant specified in the turbulence model = 0.09
- $\epsilon = C_\mu \frac{k^{\frac{3}{2}}}{l}$

Once again water is used to model the Newtonian fluid. Both k and ϵ will be used to model the turbulence.

To capture near wall effects, viscous layers in turbulent flow, there are two options available:

- **Full resolution**
  This means that near the wall the cell size is decreasing, leading to better accuracy, but longer computational time.
- **Wall function** This means the first cell from the wall is larger, as it contains the change from viscous sublayer to turbulent flow. The size of this first cell needs to be at least:

$$y^+ = \frac{y \cdot \mu_\tau}{\nu}$$

$$\text{with:}$$

$$\mu_\tau = \text{friction velocity}$$

$$y = \text{absolute distance from the wall}$$
$$\nu = \text{kinematic viscosity}$$

Reading the Darcy-Weisbach friction factor from the Moody diagram gives about 0.031 [-]. The total pressure loss according to empirical calculations becomes:

$$P = \lambda_{dw} \frac{L}{D} \frac{\rho u^2}{2} = 0.031 \frac{1}{0.01} \frac{1000 \cdot 1^2}{2} = 1550 \text{Pa}$$

Figure D.2 shows the CFD calculation of the model, with a normalized pressure drop of 1.528, which, when multiplied with the density, becomes 1528 Pa. Which is nearly the same as the empirically calculated pressure losses.
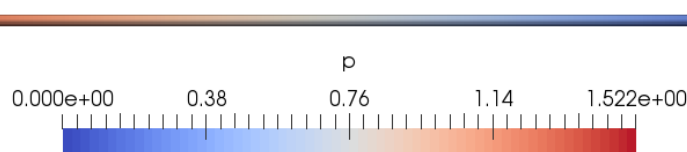
Figure D.2: Turbulent Newtonian pipeline flow over 1 meter pipe of 0.01m diameter

D.2.3. Laminar non-Newtonian

Laminar flow of a non-Newtonian mixture gave nearly identical results using the Swamee-Aggerwall [34]equation. The Swamee-Aggerwall equation is extensive, therefore reference is made to the original source.

In the CFD calculation the Herschel-Bulkley transport model is used. For an undiluted sample of Atlantis II the Herschel-Bulkley coefficients were determined to be:

$$\tau = \tau_y + K\dot{\gamma}^n$$

- $\tau_y = 14.3[\text{Pa}]$
- $K = 1.403[\text{Pa} \cdot \text{s}]^n$
- $n = 0.4[-]$ If these parameters are to be added to the transport model and the solver is an in-compressible solver, which simpleFoam is, these values have to be divided by the density, except the flow index n, so:
- $\tau_y = 0.011917[\text{Pa}]$
- $K = 0.001090833[\text{Pa} \cdot \text{s}]^n$
- $n = 0.4[-]$

Also nu0 needs to be added to the transportmodel, which stands for a minimal viscosity, as the solver computates the viscosity in the following manner:

$\nu = \min(\nu_0 , \frac{\tau_y}{\dot{\gamma}} + K \cdot \dot{\gamma}^{(n-1)})$. Eventually a λ_{dw} is found of 1277.67, which is very large. However, the idea is pushing a viscous fluid slowly through a pipeline. Using the same calculation with the Darcy-Weisbach friction coefficient as always, the following is obtained:

$$P = \lambda_{dw} \frac{L}{D} \frac{\rho u^2}{2} = 1277.67 \frac{1}{0.01} \frac{1200 \cdot 0.01^2}{2} = 7666 \text{Pa}$$

Looking at figure D.3, it shows that the normalized pressure is 6.329. Multiplying this with the density of the non-Newtonian slurry, the following is obtained:

$$P = 6.329 \cdot 1200 = 7595$$
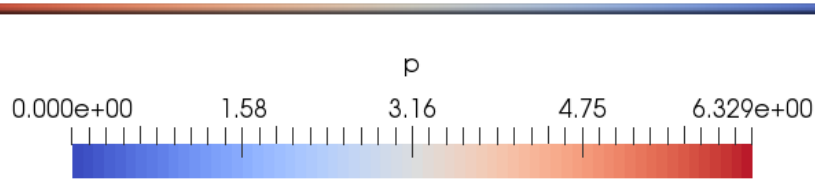
Figure D.3: Laminar non-Newtonian pipeline flow over 1 meter pipe of 0.01m diameter

D.2.4. Turbulent non-Newtonian

This is the most extensive case; combining non-Newtonian properties with turbulence. Results for this type of simulation are not reliable, as this is still a topic of research.

The Herschel-Bulkley model will be used to model the fluid. A problem with this model and the CFD software, is that a v_0 needs to be declared, which is not needed for the analytical approach.

v_0 is the viscosity at a shear rate of 0, so corresponds with solid like behaviour. Viscosity is calculated the following way: $v = \min(v_0, \frac{\tau_y}{\dot{\gamma}} + K \cdot \dot{\gamma}^{(n-1)})$. Setting v_0 too low, causes calculated values to be completely dismissed, whereas setting v_0 too high will lead to too high viscosity values and too high pressure losses.
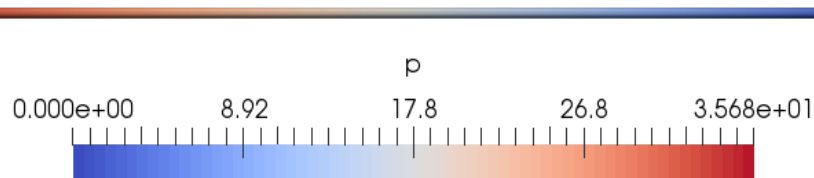
Figure D.4: Turbulent non-Newtonian pipeline flow over 1 meter pipe of 0.01m diameter

As can be seen in figure D.4, the normalized pressure loss over the length is 3.568. Multiplying this with the density, the following value is obtained: $3.568 \cdot 1200 = 42,816$ Pa.

λ obtain by the Bingham model is 0.0196, meaning the total pressure loss is:

$$P = \lambda_{\text{dw}} \frac{L}{D} \frac{\rho u^2}{2} = 0.0196 \frac{1}{0.01} \frac{1200 \cdot 5^2}{2} = 29388 \text{Pa}$$

This means a difference of 50% exists between the analytical and the CFD results. The turbulent dissipation rate (ϵ) is adjusted within the model. A too high value of v_0 leads to extremely high values of ϵ ($10^2 3$), but on the other hand v_0 needs to be as large as possible to capture high viscosity/solid like behaviour.

D.2.5. Lessons Learned

During the CFD subject, various difficulties were encountered and some were overcome, whereas others were not. Some lessons learned are:

- Solver choice is between a steady-state solver and a transient solver. A steady state solver searches for the steady solution, whereas a transient solver shows a time simulation of the flow.
  As a pipeline is modeled with a constant inflow from the inlet and a defined pressure at the outlet, a steady-state solver is used.
- To model a pipeline always use hexahedron mesh elements instead of tetrahedrons. Tetrahedrons can easily fill smaller gaps, but the shapes they acquire are random over the pipeline length, while flow through a pipeline should be a somewhat stable process. Hexahedrons lead to better results when comparing with analytical solutions.
  Using hexahedrons and a stable mesh shape over length for the pipe, also makes it much easier to make

use of a wallfunction, as the outer mesh element can be dimensioned to capture the viscous layer near the wall.

- There are two models for turbulence for the RANS turbulence model: the k-ϵ and the k-ω model. Both models lead to good convergence on the laminar Newtonian solution. For these tests, k-ϵ was used, the k-ω model just requires one more analytical calculation step.

- To see if certain model setup works, it is advisable to use a coarse mesh and use low relative tolerance for the solvers. This consumes the least amount of time and an idea will be obtained whether the solution will be acceptable.

- Using a wall function is preferable over a full resolution as this saves a lot of time. A full resolution simulation uses a lot of small cells near the wall, whereas using a wall function declares different boundaries within the one cell closest to the wall, where the wall function is specified. Still, using the wall function on a pretty coarse mesh still takes about 15 minutes.

- For incompressible flow, see table D.1 and D.2 to see stability of the solver for different boundary conditions.

Table D.1: Stability of CFD calculation for different boundary conditions for pressure or velocity on the inlet and outlet

Inlet		Outlet		Stability
Physics	**OpenFOAM**	**Physics**	**OpenFOAM**	
Volume flow rate	flowRateVelocity	Static pressure	fixedValue	Excellent
Total pressure	totalPressure	Total pressure	totalPressure	Very Good
Total pressure	totalPressure	Static pressure	fixedValue	Good
Static pressure	fixedValue	Static pressure	fixedValue	Poor

Table D.2: Stability of CFD calculation for different boundary conditions for return flow on the inlet and outlet

Type	Condition	Stability
Outflow	zeroGradient	Unstable, if flow reverses
Blocked	inletOutlet	Good, but nonphysical
Return flow I	pressureInletOutlet	Good
Return flow II	totalPressure	Very Good

In these tests, defined velocity at the inlet and a fixedValue of zero pressure at the outlet were used. The choice of boundaries depends of course on what is relevant for the real life case or how this can be approached in the best way possible.

E

Morphological Overview Tables of the concepts

Pumps	Positive Displacement Pumps		Centrifugal Pumps	
Soil activation - method	Jetting	Cutting		Stirring
Dilution	Jetting	Hose to sea water	Hose to brine	Brine from location
Start-up / Phase-out procedure	Flush Pipeline		Install extra pumping power	
Coverage of scope	Moveable suction pipes	Moveable equipment		Expandable system
Flow assurance	Laminar flow	Transition region		Turbulent flow
Transport line position	On the sea bed to the mud layer	On the sea bed to the brine layer	Floating above the mud layer	Floating above the brine layer
Transport line maneuverability	Stationary	Floating, moved by winches attached to anchors		Floating, moved by thrusters
Soil activation - equipment	Pipeline activation	Floating hose equipment	Floating equipment	Surface crawler
Filtering	No filtering	Filter particles that can not be transported		Filter particles that are not of interest
Filtering Position	Front of the suction pipe	Inside the suction pipe	Multiple locations in the suction pipe	Outside the pipe (hydrocyclone)

Figure E.1: Morphological Overview Table - Flexible Suction Hose Concept

Pumps	Positive Displacement Pumps			Centrifugal Pumps		
Soil activation - method	Jetting		Cutting			Stirring
Dilution	Jetting	Hose to sea water		Hose to brine		Brine from location
Start-up / Phase-out procedure	Flush Pipeline			Install extra pumping power		
Coverage of scope	Moveable suction pipes	Moveable equipment			Expandable system	
Flow assurance	Laminar flow		Transition region		Turbulent flow	
Transport line position	On the sea bed to the mud layer	On the sea bed to the brine layer		Floating above the mud layer	Floating above the brine layer	
Transport line maneuverability	Stationary	Floating, moved by winches attached to anchors			Floating, moved by thrusters	
Soil activation - equipment	Pipeline activation	Floating hose equipment	Floating equipment			Surface crawler
Filtering	No filtering	Filter particles that can not be transported			Filter particles that are not of interest	
Filtering Position	Front of the suction pipe	Inside the suction pipe	Multiple locations in the suction pipe		Outside the pipe (hydrocyclone)	

Figure E.2: Morphological Overview Table - Floating Platform Concept

Pumps	Positive Displacement Pumps		Centrifugal Pumps		
Soil activation - method	Jetting	Cutting			Stirring
Dilution	Jetting	Hose to sea water		Hose to brine	Brine from location
Start-up / Phase-out procedure	Flush Pipeline		Install extra pumping power		
Coverage of scope	Moveable suction pipes	Moveable equipment		Expandable system	
Flow assurance	Laminar flow	Transition region		Turbulent flow	
Transport line position	On the sea bed to the mud layer	On the sea bed to the brine layer		Floating above the mud layer	Floating above the brine layer
Transport line maneuverability	Stationary	Floating, moved by winches attached to anchors		Floating, moved by thrusters	
Soil activation - equipment	Pipeline activation	Floating hose equipment	Floating equipment		Surface crawler
Filtering	No filtering	Filter particles that can not be transported		Filter particles that are not of interest	
Filtering Position	Front of the suction pipe	Inside the suction pipe	Multiple locations in the suction pipe	Outside the pipe (hydrocyclone)	

Figure E.3: Morphological Overview Table - Expandable Pipe Concept

Pumps	Positive Displacement Pumps		Centrifugal Pumps		
Soil activation - method	Jetting		Cutting		Stirring
Dilution	Jetting	Hose to sea water	Hose to brine		Brine from location
Start-up / Phase-out procedure	Flush Pipeline		Install extra pumping power		
Coverage of scope	Moveable suction pipes		Moveable equipment		Expandable system
Flow assurance	Laminar flow		Transition region		Turbulent flow
Transport line position	On the sea bed to the mud layer	On the sea bed to the brine layer		Floating above the mud layer	Floating above the brine layer
Transport line maneuverability	Stationary	Floating, moved by winches attached to anchors			Floating, moved by thrusters
Soil activation - equipment	Pipeline activation	Floating hose equipment	Floating equipment		Surface crawler
Filtering	No filtering		Filter particles that can not be transported		Filter particles that are not of interest
Filtering Position	Front of the suction pipe	Inside the suction pipe	Multiple locations in the suction pipe		Outside the pipe (hydrocyclone)

Figure E.4: Morphological Overview Table - Horizontal Trawler Concept